

# Testing the Provenance of Santonian- Maastrichtian lobe of the Ceduna Delta

Thesis submitted in accordance with the requirements of the University of  
Adelaide for an Honours Degree in Geology

Jarred Cain Lloyd  
November 2014



THE UNIVERSITY  
*of* ADELAIDE

**TITLE**

Testing the Provenance of Santonian-Maastrichtian lobe of the Ceduna Delta

**RUNNING TITLE**

Provenance of the Upper Ceduna Delta Lobe

**ABSTRACT**

The Ceduna Delta represents a vast Cretaceous stacked delta system located in the Bight Basin and is currently the focus of considerable petroleum exploration. Two competing models have been suggested for the source of the upper Santonian-Maastrichtian delta lobe. Originally, it was proposed that both the upper and lower lobes of the delta were sourced from the Australian Eastern Highlands via a continent scale river. A recent study suggested that the two lobes had different sources, with the upper lobe instead being sourced proximally from the western Eromanga Basin and within present day South Australia. This new model was primarily based on existing and new, but sparse apatite fission track data. This study tested the two competing models, by comparing the detrital zircon U/Pb age distribution and Lu-Hf isotopic composition of samples from the Late Cretaceous Winton Formation in the eastern Eromanga Basin (part of the proposed source of the upper Ceduna delta) with samples from the Gnarlyknots-1A well within the Ceduna Sub-basin of the Bight Basin. Zircon U/Pb data and hafnium isotopic data from the Gnarlyknots-1A well and eastern Eromanga Winton Formation demonstrates the similarity in provenance of the two formations and that both ultimately are sourced from the Australian Eastern Highlands.

**KEYWORDS**

Provenance, U-Pb Age, Hafnium Isotopes, Geochemistry, Ceduna Delta, Bight Basin

## TABLE OF CONTENTS

Title.....	I
Running title .....	I
Abstract.....	I
Keywords.....	I
Table of Contents .....	II
List of Figures and Tables .....	IV
Introduction .....	1
Background.....	6
Geological Setting.....	7
Bight Basin.....	7
Eromanga Basin .....	9
Methods .....	10
Observations and Results .....	12
Existing U-Pb detrital zircon data .....	12
Gnarlyknots-1A Sample 74317 (data from MacDonald et al. (2013b)).....	12
Gnarlyknots-1A Sample 74318 (data from MacDonald et al. (2013b)).....	12
Gnarlyknots-1A Sample 74319 (data from MacDonald et al. (2013b)).....	13
Gnarlyknots-1A Sample 74320 (data from MacDonald et al. (2013b)).....	13
Gnarlyknots-1A Sample 74321 (data from MacDonald et al. (2013b)).....	14
Gnarlyknots-1A Sample 74323 (data from MacDonald et al. (2013b)).....	14
Gnarlyknots-1A Sample 74324 (data from MacDonald et al. (2013b)).....	14
Gnarlyknots-1A Sample 74325 (data from MacDonald et al. (2013b)).....	15
Gnarlyknots-1A Sample 74326 (data from MacDonald et al. (2013b)).....	15
Winton Formation Samples 8622-61 and 8642-168 (data from MacDonald and Holford pers. comm. 2014).....	18
Eromanga-1 (Data from Tucker et al. (2013)).....	20
Isisford (Data from Tucker et al. (2013)) .....	20
Lark Quarry Conservation Park (Data from Tucker et al. (2013)).....	20
Bladensburg National Park (Data from Tucker et al. (2013)).....	21
Longreach-1 (Data from Tucker et al. (2013)) .....	21
Hughes-2 Sample 1069106 (data from MacDonald and Holford pers. Comm. 2014) .....	23
Hughes-2 Sample 1069111 (data from MacDonald and Holford pers. Comm. 2014) .....	24
New U-Pb Data .....	25
Gnarlyknots-1A Sample 74322 .....	25

Hughes-2 Sample 106988 .....	26
Gnarlyknots-1A Hafnium Analyses .....	27
Discussion.....	29
Maximum Depositional Ages.....	29
U-Pb Age Provenance of the Cretaceous in South Australia .....	31
Hafnium Isoptic Constraints on the Provenance of the Ceduna Sub-Basin .....	36
Conclusions .....	38
Acknowledgments .....	39
References .....	40
Appendix A: Detailed Methods.....	42
Uranium-Lead Geochronology.....	42
Hafnium Isotopic Analysis .....	42
Appendix B: NEW U-Pb and Hf Isotope Data.....	44

## LIST OF FIGURES AND TABLES

Figure 1: Location of Gnarlyknots-1A drill hole, Hughes-2 drill hole, the Ceduna sub-basin and Gnarlyknots-1A sample depths .....	1
Figure 2: Map of Australia showing the locations where uranium-lead and hafnium isotope data was sourced, major basins of Australia coloured according to age. The black box represents the inset for Figure 1. The major basins of interest, the Eromanga and Bight Basins, are outlined in black. ....	5
Figure 3: Bight Basin correlation chart showing link between the sea level curve, lithostratigraphy, sequence stratigraphy and basin phases. After Totterdell et al. (2003)	8
Figure 4: Stratigraphic chart of the Eromanga Basin showing the relationship to sea level curve. After Cotton et al. (2006b).....	10
Figure 5A-J: Uranium-lead Concordia plots showing all data for each Gnarlyknots-1A sample with corresponding kernel density estimate (green shading, adaptive bandwidth), probability density plot (black line) and histogram (grey boxes, net frequency on Y-axis, 100 Ma bin width) using 90-110 concordant data with each datum represented by a black circle on the X-axis. ....	18
Figure 6A&B: Uranium-lead Concordia plots showing all data for two western Eromanga basin samples from Dullingari-1 and Burely-2 drill holes with corresponding kernel density estimate (green shading, adaptive bandwidth), probability density plot (black line) and histogram (grey boxes, net frequency on Y-axis, 100 Ma bin width) using 90-110 concordant data with each datum represented by a black circle on the X-axis.....	19
Figure 7A-E: Uranium-lead Concordia plots showing all data for five central and eastern Eromanga basin samples with corresponding kernel density estimate (green shading, adaptive bandwidth), probability density plot (black line) and histogram (grey boxes, net frequency on Y-axis, 100 Ma bin width) using 90-110 concordant data with each datum represented by a black circle on the X-axis.....	23
Figure 8A&B: Uranium-lead Concordia plots showing all data for Hughes-2 drill hole samples 109106 and 1069111 with corresponding kernel density estimate (green shading, adaptive bandwidth), probability density plot (black line) and histogram (grey boxes, net frequency on Y-axis, 100 Ma bin width) using 90-110 concordant data with each datum represented by a black circle on the X-axis.....	24
Figure 9A&B: Uranium-lead Concordia plots showing new uranium-lead data (A) and previous data from MacDonald et al. (2013b) (B) for Gnarlyknots-1A sample 74322 with corresponding kernel density estimate (green shading, adaptive bandwidth), probability density plot (black line) and histogram (grey boxes, net frequency on Y-axis, 100 Ma bin width) using 90-110 concordant data with each datum represented by a black circle on the X-axis. ....	26
Figure 10: Uranium-lead Concordia plots showing all data for Hughes-2 sample 106988 with corresponding kernel density estimate (green shading, adaptive bandwidth), probability density plot (black line) and histogram (grey boxes, net frequency on Y-axis, 100 Ma bin width) using 90-110 concordant data with each datum represented by a black circle on the X-axis. ....	27

Figure 11: Plot showing epsilon hafnium in relation to uranium-lead age of Gnarlyknots-1A zircon samples. A chondritic uniform reservoir reference line (purple) plots along (x, 0), the epsilon hafnium depleted mantle line (aqua) shows the modelled mantle epsilon hafnium values and the epsilon hafnium new crust line (grey) shows the new epsilon hafnium mantle model values as suggested by Dhuime et al. (2011). The epsilon hafnium values provide information about the material that melted to form the magma from which the zircon crystallised. Negative epsilon hafnium values indicate involvement of existing continental crust in magma genesis; conversely positive epsilon hafnium values indicate the source had experienced a prior depletion event. Data points below the chondritic uniform reservoir are considered evolved, above the depleted mantle are highly depleted and between the chondritic uniform reservoir and depleted mantle are considered juvenile. The kernel density estimate (green shaded area) and probability density plot (black solid line) are overlain for visual correlation of zircon populations. .... 29

Figure 12 A-D: Maximum depositional ages determined by the youngest near concordant  $U^{238}/Pb^{206}$  age errors plotted at the  $2\sigma$  level, for: (A) Mackunda Formation (Longreach-1), and Winton Formation, (B) Loongana Formation from Hughes-2 and (C) Potoroo Formation (GN 74317-74319) and Wigunda Formation (GN 74320-74326). A slight trend of decreasing age (using only  $<160$  Ma,  $<10\%$  discordant zircons) with increasing sample depth for the Gnarlyknots-1A samples is shown in (D). This suggests progressive erosion of a normally layered sedimentary succession. .... 31

Figure 13: Combined display of zircon uranium-lead ages for Hughes-2, Bight Basin, showing histogram (grey rectangles, net frequency shown on Y-axis, bin-width of 100), kernel density estimate (green shading, adaptive bandwidth) and probability distribution plot (black line). Each datum is represented by a black circle on the X-axis..... 32

Figure 14: Combined display of zircon uranium-lead ages for Winton Formation samples, showing histogram (grey rectangles, net frequency shown on Y-axis, bin-width of 100), kernel density estimate (green shading, adaptive bandwidth) and probability distribution plot (black line). Each datum is represented by a black circle on the X-axis ..... 33

Figure 15: Combined display of zircon uranium-lead ages for Gnarlyknots-1A, Ceduna Sub-basin, showing histogram (grey rectangles, net frequency shown on Y-axis, bin-width of 100), kernel density estimate (green shading, adaptive bandwidth) and probability distribution plot (black line). Each datum is represented by a black circle on the X-axis..... 35

Figure 16: Corrected  $\epsilon Hf$  values for Gnarlyknots-1A, the Rakaia Terrane in New Zealand (Acott 2013), the Musgrave Province (Smithies et al. 2011, Kirkland et al. 2013) and the Mount Painter Province (Kromkhun et al. 2013). .... 37

Supplementary Table 1: U-Pb data collected for Gnarlyknots-1A sample 74322 ..... 44

Supplementary Table 2: U-Pb data collected for Hughes-2 sample 106988..... 46

Supplementary Table 3: Hf data collected for gnarlyknots-1A, sample 74318 ..... 48

Supplementary Table 4: Hf data collected for Gnarlyknots-1A, sample 74319 ..... 49

Supplementary Table 5: Hf data collected for Gnarlyknots-1A, sample 74321 ..... 50

Supplementary Table 6: Hf data collected for Gnarlyknots-1A, sample 74322 ..... 51

Supplementary Table 7: Hf data collected for Gnarlyknots-1A, sample 74323 ..... 52  
Supplementary Table 8: Hf data collected for Gnarlyknots-1A, sample 74326 ..... 53

## INTRODUCTION

The Ceduna Sub-basin (Figure 1) is one of eight depocentres in the large Bight Basin off the southern Australian coast. It contains two deltaic sequences that are represented by the Hammerhead Supersequence, which contains the Potoroo and Wigunda formations, and the White Pointer Supersequence, containing the Platypus formation.

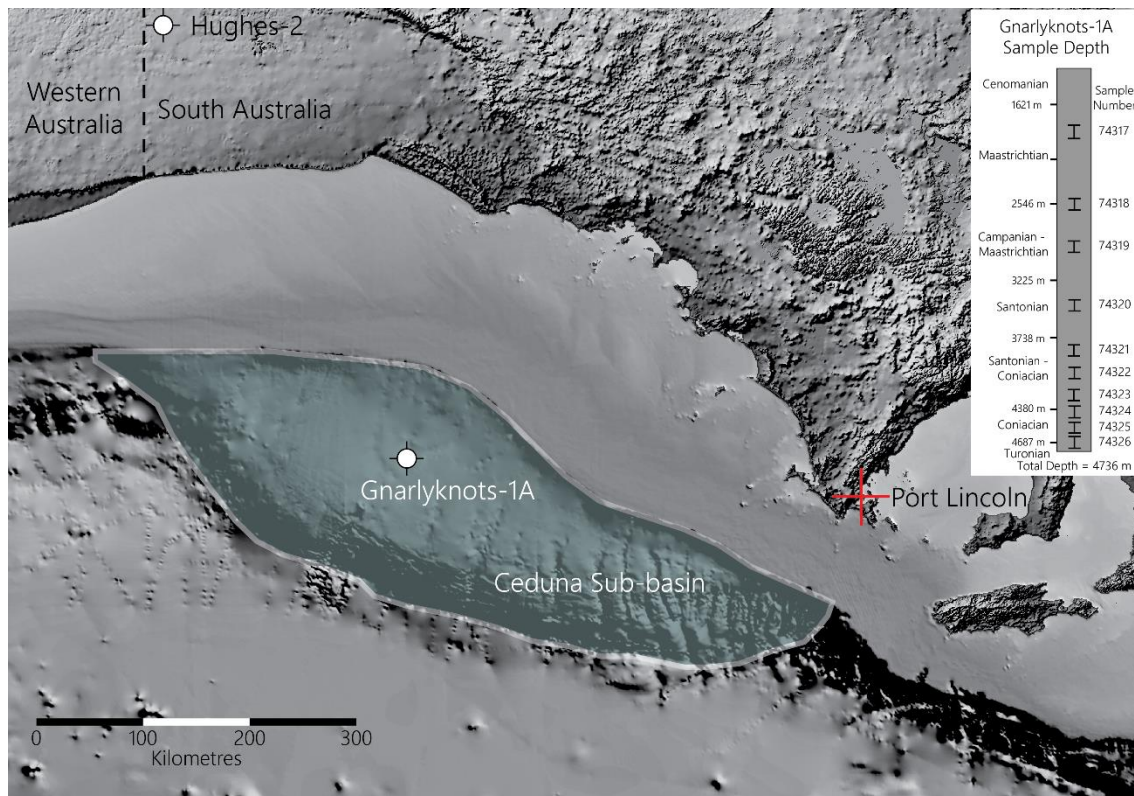


**Figure 1: Location of Gnarlyknots-1A drill hole, Hughes-2 drill hole, the Ceduna sub-basin and Gnarlyknots-1A sample depths**

These supersequences have formed a very large and conspicuous bathymetric expression, colloquially referred to as the Ceduna Delta. Although this delta is as large as the modern Niger Delta, and has high petroleum prospectivity (King and Mee 2004), very little is known about the origin, source and demise of the delta (MacDonald et al. 2013b). This is primarily due to the lack of exploration wells, and thus access to samples, because of the delta being located in a high-risk area. Extensive seismic and



structural analyses have been conducted on the Ceduna Sub-basin, identifying two structurally and temporally separated delta lobes (Totterdell et al. 2003, MacDonald et al. 2013a). The older Cenomanian lobe (100.5-93.9 Ma) contains the White Pointer Supersequence (Totterdell et al. 2003) and the younger Santonian-Maastrichtian (86.3-72.1 Ma) lobe, mainly consists of the Hammerhead Supersequence (Totterdell et al. 2003).

The source of the delta sediments is currently not well understood. Initial models indicated a provenance in northeast Australia (Veevers 2000, King and Mee 2004). However, MacDonald et al. (2013b) conducted a provenance study using U-Pb geochronology on detrital zircons sampled from the Gnarlyknots-1 exploration well and their results provided evidence that led them to propose an alternative model where the Santonian-Maastrichtian sediments of the Ceduna Delta are sourced more proximally, from within present-day South Australia, and not from a trans-continental river system as theorised earlier.

Although U-Pb geochronology on detrital zircons has been widely used for provenance and is generally effective, it has become increasingly realised that provenance studies solely based on zircon U-Pb ages are limiting, as zircon growth events may not be unique to specific terranes (Howard et al. 2009). Additional isotopic constraints, such as Lu-Hf data, may overcome this issue by providing a separate, independent, data set to compare detritus with source terrane. The MacDonald et al. (2013b) study demonstrates this limitation, whereby two possible spatially distant source regions are suggested for a population of zircons; however, there is little supplementary evidence that assists in the determination of which source region is more probable. As such, further investigation is

required to gain a more detailed and accurate understanding of the origin of the Ceduna Delta.

Based on detrital apatite fission track data MacDonald et al. (2013b) suggested that a regional arcuate-shaped exhumation event encompassing the southern Musgrave Block, western Eromanga Basin, Officer Basin, Flinders Ranges, Yorke Peninsula, Southern Adelaide Fold Belt and Kangaroo Island began between 100 and 80 Ma. This late Cretaceous exhumation event is suggested to have resulted in 1-2 kilometres of erosion providing a source of Permian, Jurassic and Cretaceous detritus. In combination with the suggested exhumation event, the seismic character of the delta, specifically high-angle bedforms that are interpreted to indicate rapid deposition, is used to reason the upper delta lobe was sourced more proximally than previously suggested. It must be noted, however, that in situ fission track data is absent from much of the inland parts of this proposed uplift area, so much inference had to be made using data from coastal Australia.

This study has concentrated on providing new zircon Lu-Hf data from previously studied core samples of both the Ceduna Sub-Basin, the Loongana Formation of the Madura Shelf and from the Winton Formation in the Eromanga Basin where U-Pb data had already been obtained (MacDonald et al. 2013a; Justin MacDonald and Simon Holford personal communication) to better understand the provenance and evolution of the source areas to these regions and to test their similarities as whether they are feasibly part of the same sedimentary system. Previously collected U-Pb data (both published and unpublished) were (re)processed and newly plotted. In addition, new U-Pb data were collected from two samples to complement the existing datasets. In particular, I test whether the Santonian-Maastrichtian delta lobe is distally sourced from

the Australian Eastern Highlands by a continental scale southeast flowing river, instead of the more proximal Adelaide Rift Complex and western Eromanga Basin as suggested by MacDonald et al. (2013b). The source of the Ceduna Delta sediments has implications on the reservoir rock quality and; therefore, gaining a better understanding of the source and evolution of the Ceduna Delta has implications on petroleum exploration within the Ceduna Sub-basin, and Bight Basin. It will also provide further insight into the paleogeography of Australia, by reconstructing part of the fluvial system in Australia in the Late Cretaceous.



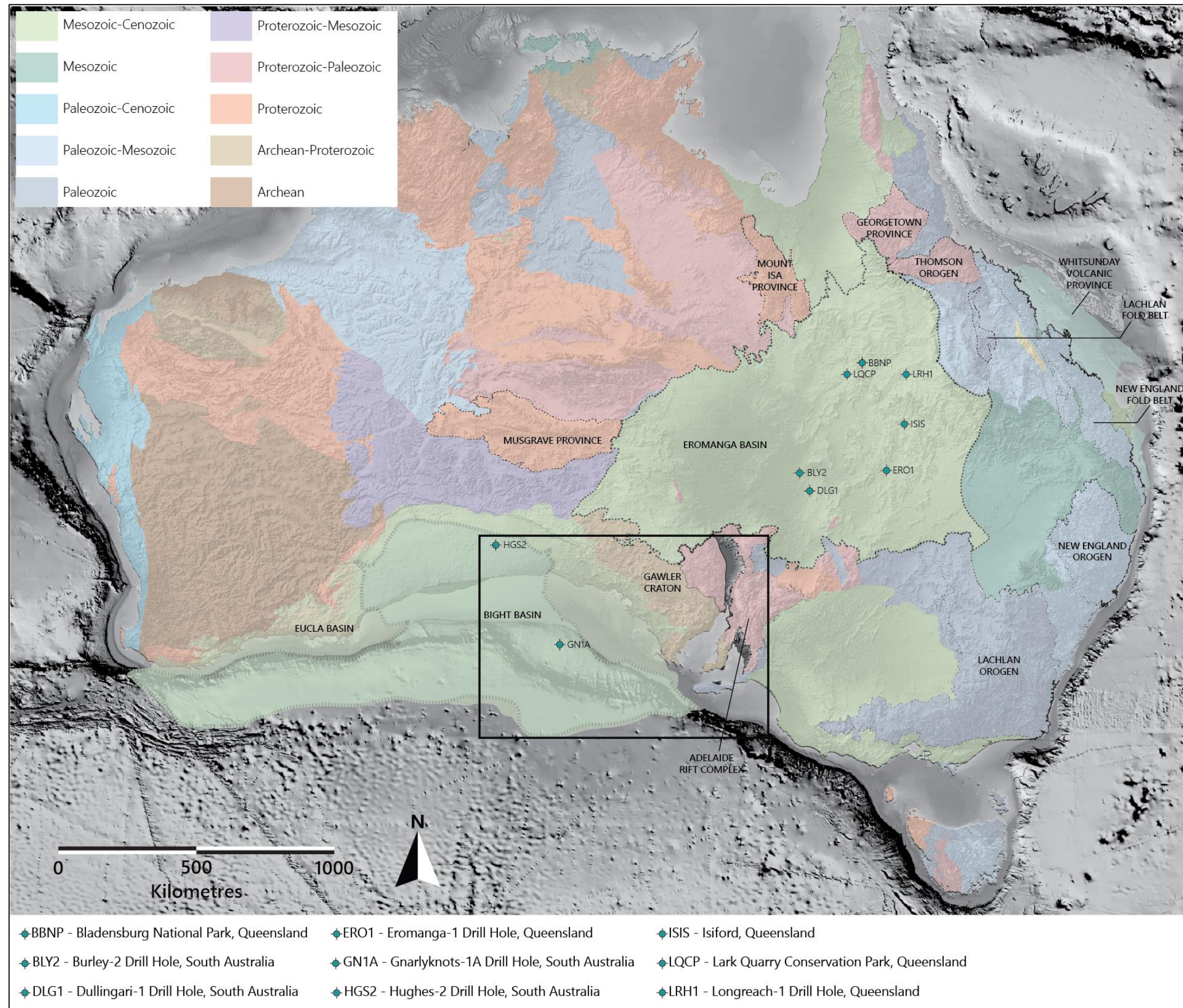


Figure 2: Map of Australia showing the locations where uranium-lead and hafnium isotope data was sourced, major basins of Australia coloured according to age. The black box represents the inset for Figure 1. The major basins of interest, the Eromanga and Bight Basins, are outlined in black.



## **BACKGROUND**

It has been widely theorised, though neither proved nor disproved, that the Ceduna Delta sediments were deposited by a continent-scale south-west flowing river system. In these models, the primary source of detritus in the Ceduna delta is thought to be either erosional detritus from the Eromanga basin (King and Mee 2004) or the Australian Eastern Highlands (Veevers 2000, Krassay and Totterdell 2003). In particular the late Albian-Cenomanian Winton Formation sediments (Tucker et al. 2013) yield similar zircon age characteristics to the younger, Santonian-Maastrichtian, sedimentary rocks of the upper Ceduna Delta. MacDonald et al. (2013b) recently published new detrital zircon uranium-lead (U-Pb) age data from samples obtained from the Gnarlyknots-1A drill hole. Their findings challenge this theory, and suggest that, at the least, the sediments from the younger Santonian-Maastrichtian lobe of the delta have a more proximal provenance than previously anticipated. The proximal model was suggested based primarily on the seismic characteristics of the delta and a suggested broad, late Cretaceous exhumation event thought to have restricted the catchment area. The U-Pb and fission-track zircon data obtained by MacDonald et al. (2013b) for the Gnarlyknots-1A drill core provided the sole constraints on the provenance of the deltaic sediments. As noted in MacDonald et al. (2013b) no well with available samples has penetrated the older, Cenomanian aged, lobe of the Ceduna Delta. The Potoroo-1 well was abandoned at 2924 m, in what is described as the equivalent of the Pretty Hill and Geltwood Beach (Eumeralla) formations ("Shell" 1975) and Gnarlyknots-1A abandoned at 4736 m (Willis 2003) in the Wigunda Formation, meaning that the source of the Cenomanian delta lobe can only be speculated.

## **Geological Setting**

Of particular importance to this study are the Ceduna Sub-basin and the Cretaceous sediments of the Eromanga Basin, which are thought to be a potential source rocks for the upper Ceduna Delta lobe. The following section discusses the sedimentary records of both the Ceduna and Eromanga basins, aiming to understand their potential relationship in the provenance model.

## **BIGHT BASIN**

Formation of the Bight Basin occurred in two successive periods of extension and thermal subsidence commencing in the Middle to Late Jurassic (Totterdell et al. 2003), with the Middle Cretaceous extensional phase being associated with the Late Santonian break-up of Australia and Antarctica (Totterdell et al. 2003, MacDonald et al. 2013b). Between the Jurassic and Early Cretaceous, the Bight Basin contains dominantly non-marine sediments. However, from the late Aptian until the end of the Cretaceous, deposition occurred in marine and deltaic environments. The relationships between basin phases, lithostratigraphy, sequence stratigraphy and time are shown in Figure 3.

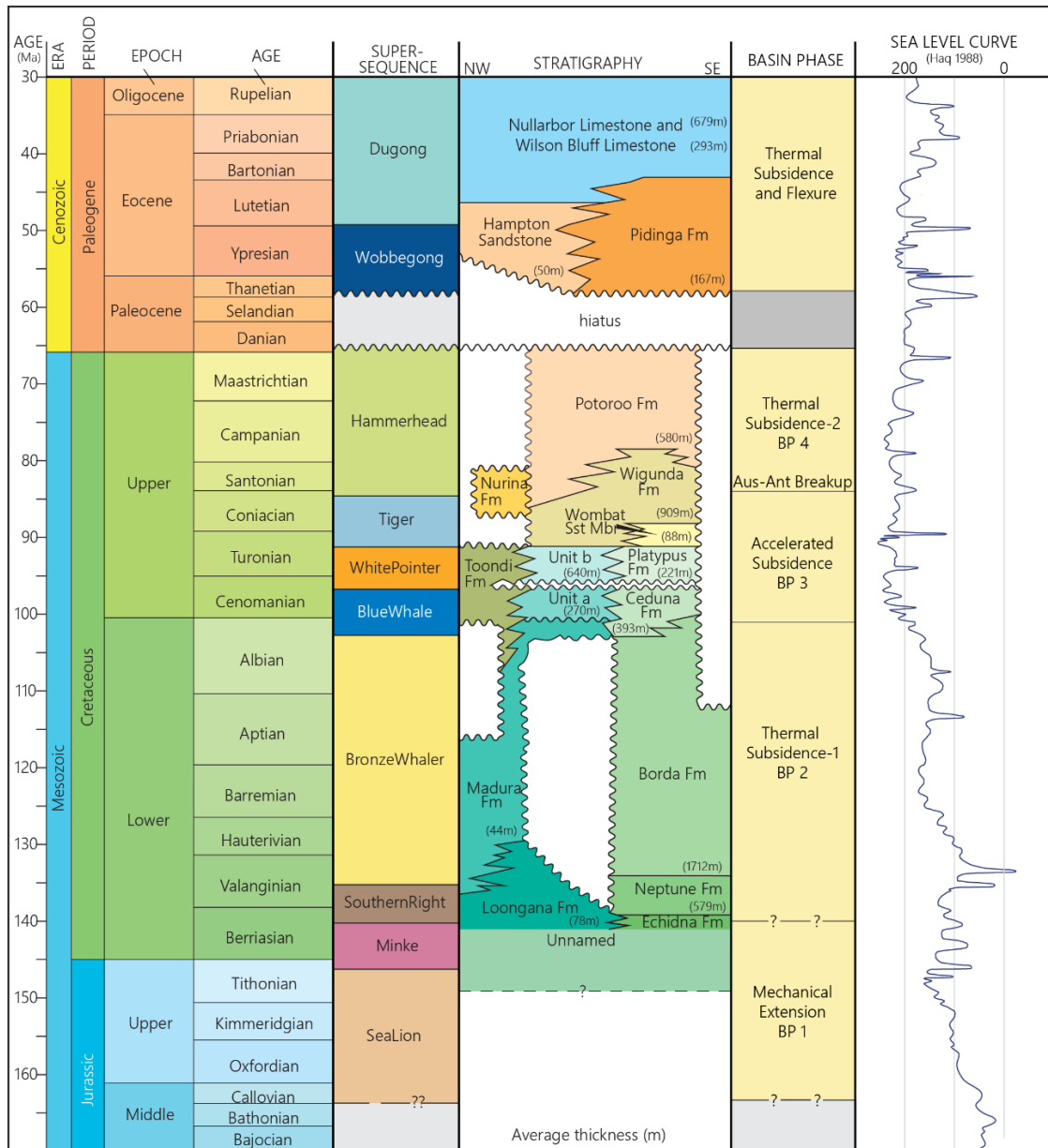


Figure 3: Bight Basin correlation chart showing link between the sea level curve, lithostratigraphy, sequence stratigraphy and basin phases. After Totterdell et al. (2003)

### Ceduna Sub-Basin

The west-northwest trending Ceduna Sub-basin (Figure 1) is the major depocentre of the Bight Basin and is the largest of the sub-basins in the Bight Basin. The sub-basin consists of middle Jurassic to Late Cretaceous sedimentary rocks that locally exceed 12 km in total thickness (Totterdell et al. 2003, MacDonald 2013). The Ceduna Sub-basin lies beneath the distinctly visible Ceduna Terrace with water depths between 200 and

5200 m. It is characterised by two periods of deltaic progradation, an Albian-Cenomanian delta and a Santonian-Maastrichtian lobe. The structural architecture of the Albian-Cenomanian delta consist of a system of gravity-driven, detached extensional and contractional faults and mud diapirism (Totterdell et al. 2003). The primary deltaic sediments that form the distinct Ceduna Delta of the Ceduna Sub-basin are the White Pointer and Hammerhead supersequences (Totterdell et al. 2003, MacDonald 2013) The Late Santonian-Maastrichtian delta is a sand-rich system featuring strongly progradational stratal geometries and includes simple planar normal faults (Totterdell et al. 2003). Both deltaic systems contain potential structural and stratigraphic traps, with the later Santonian-Maastrichtian delta containing especially good potential hydrocarbon reservoirs.

#### EROMANGA BASIN

The Mesozoic Eromanga Basin is a large oil and gas producing, intracratonic sedimentary basin covering a large portion of northeast central Australia. Overlying the Permo-Carboniferous Arckaringa, Cooper and Pedirka Basins (Cotton et al. 2006a). Deposition in the Eromanga Basin was relatively continuous and widespread throughout the Early Jurassic to Late Cretaceous, controlled by subsidence rates and plate tectonic events on the Australia Plate margins (Cotton et al. 2006a). The sedimentary record of the Eromanga Basin can be divided into three packages: lower non-marine, marine and upper non-marine. Of particular importance for this study are the upper non-marine formations, primarily the coal bearing Winton Formation, but also to a lesser extent the Cadna-owie Formation and Mackunda Formation, (and “Mt Howie Sandstone”) as they provide potential source lithologies, with a similar age as for the Ceduna Delta sedimentary rocks.



## Winton Formation

The Winton Formation is described as being interbedded fine to coarse-grained sandstone, carbonaceous and pyritic shale, siltstone and coal seams with intraclast conglomerates (Cotton et al. 2006a). The sandstone beds contain abundant fresh volcanogenic debris, as well as lithics, feldspar, and traces of apatite, mica and ferromagnesian minerals. It is Late Albian-Cenomanian in age (Cotton et al. 2006a, Tucker et al. 2013), making it of similar age as the lower delta in the Ceduna Sub-Basin. Many macrofossils are present in the formation. The thickness of the formation varies, but is generally greater than 400 m, up to 1200 m (Cotton et al. 2006a, Alley et al. 2011).

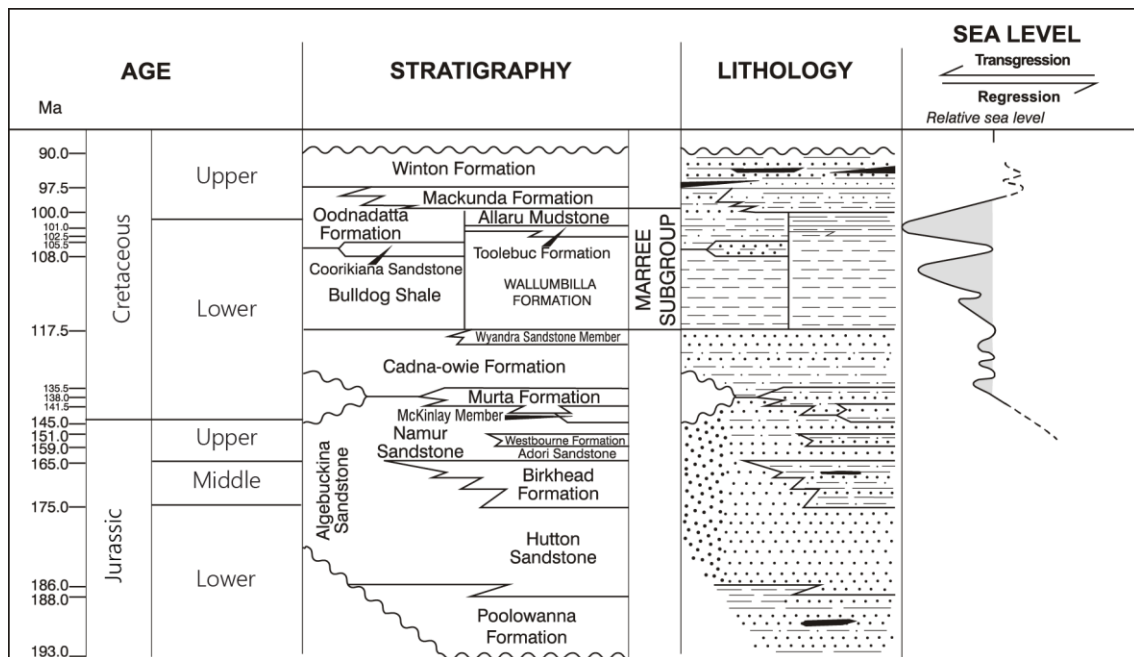


Figure 4: Stratigraphic chart of the Eromanga Basin showing the relationship to sea level curve. After Cotton et al. (2006b)

## METHODS

The main part of the project involved Hf isotopic analyses that were conducted via Laser Ablation Multi-Collector Inductively Coupled Plasma Mass Spectrometry (LA-MC-ICP-MS) on selected samples from the Gnarlyknots-1A core, from which U-Pb age

data had previously been obtained (MacDonald et al. 2012a). These data are shown in supplementary tables 3-8. A Thermo-Scientific Neptune Multi-Collector Inductively Coupled Plasma Mass Spectrometer attached at a New Wave UP193 Excimer laser located at a joint University of Adelaide and Commonwealth Scientific and Industrial Research Organisation (CSIRO) facility at the University of Adelaide's Waite Campus was used for the Hf isotopic analysis. Data processing was completed using a macro-driven Excel™ workbook, HfTRaX V3.2, written by Dr. Justin Payne. Epsilon Hf, Hf<sub>i</sub> and hafnium model ages were calculated using a modified Excel™ workbook originally developed by the ARC National Key Centre for Geochemical Evolution and Metallogeny of Continents (GEMOC) at Macquarie University, Sydney.

Additional samples were analysed for U-Pb geochronology via a Laser Ablation Inductively Coupled Plasma Mass Spectrometry (LA-ICP-MS) using a New Wave UP-213 laser attached to an Agilent 7500cx Inductively Coupled Plasma Mass Spectrometer (ICP-MS) at Adelaide Microscopy, the University of Adelaide. Zircons were imaged under cathodoluminescence prior to U-Pb analysis by previous researchers. Age calculations and corrections were completed using the software GLITTER with use of the primary zircon standard GJ-1, TIMS normalization data  $^{207}\text{Pb}/^{206}\text{Pb} = 608.3 \text{ Ma}$ ,  $^{206}\text{Pb}/^{238}\text{U} = 600.7 \text{ Ma}$  and  $^{207}\text{Pb}/^{235}\text{U} = 602.2 \text{ Ma}$  (Jackson et al. 2004). Instrument drift was also corrected for in GLITTER via standard bracketing every 15-20 unknowns and application of a linear correction. Accuracy of the methodology was verified by repeat analysis of Plešovice zircon,  $^{206}\text{Pb}/^{238}\text{U} = 337.13 \pm 0.37$  (Sláma et al. 2008). Isotope ratios are presented uncorrected for common lead, with Concordia plots generated using Isoplot 4.15.

Kernel density estimates, probability density plots and histograms were all plotted using Density Plotter, a java program developed by and described in Vermeesch (2012). An adaptive bandwidth was used for the kernel density estimates. A fixed age range of 0-3500 Ma and histogram bin width of 100 Ma was used for consistency across all plots. Data used was  $\pm 10\%$  concordant.

Detailed methods are shown in Appendix A and the raw U-Pb and Hf isotope data are shown in Appendix B.

## **OBSERVATIONS AND RESULTS**

### **Existing U-Pb detrital zircon data**

GNARLYKNOTS-1A SAMPLE 74317 (DATA FROM MACDONALD ET AL. (2013B))

This sample was sourced from the Potoroo Formation. In this sample five discrete age populations were observed (Figure 5A), the most significant population ca. 400-100 Ma zircons contained 38 (52.1%) of the <10% discordant grains. The next major population of 19 zircons (26.2%) had ages ranging from ca. 690-490 Ma. The remaining populations ca. 1255-960, 1940-1370 and 2340-2120 Ma contained 7 (9.5%), 7 (9.5%) and 2 (2.7%) zircons respectively. The youngest <10% discordant  $U^{238}/Pb^{206}$  age is  $103.5 \pm 4.7$  Ma (Lower Cretaceous, Albian) and is taken as the maximum depositional age.

GNARLYKNOTS-1A SAMPLE 74318 (DATA FROM MACDONALD ET AL. (2013B))

This sample was sourced from the Potoroo Formation. In this sample six discrete age populations were observed (Figure 5B), the most significant population ca. 370-98 Ma zircons contained 26 (46.4%) of the <10% discordant grains. The next major population

of 19 zircons (33.9%) had ages ranging from ca. 775-465 Ma. The remaining populations ca. 1030-960, 1145-1140, 1445 and 1740 Ma contained 7 (12.5%), 2 (3.6%), 1 (1.8%) and 1 (1.8%) zircon(s) respectively. The youngest <10% discordant  $U^{238}/Pb^{206}$  age is  $98.9\pm 2.0$  Ma (Upper Cretaceous, Cenomanian) and is taken as the maximum depositional age.

GNARLYKNOTS-1A SAMPLE 74319 (DATA FROM MACDONALD ET AL. (2013B))

This sample was also sourced from the Potoroo Formation. In this sample eight discrete age populations were observed (Figure 5C), the most significant population ca. 340-100 Ma zircons contained 26 (44.1%) of the <10% discordant grains. The next major population of 16 zircons (27.1%) had ages ranging from ca. 690-450 Ma. The remaining populations ca. 790-770, 965-900, 1300-1060, 1570-1445, 1900 and 2860 Ma contained 2 (3.4%), 2 (3.4%), 8 (13.6%), 3 (5.1%), 1 (1.7%) and 1 (1.7%) zircon(s) respectively. The youngest <10% discordant  $U^{238}/Pb^{206}$  age is  $100.6\pm 2.4$  Ma (Lower Cretaceous, Albian) and is taken as the maximum depositional age.

GNARLYKNOTS-1A SAMPLE 74320 (DATA FROM MACDONALD ET AL. (2013B))

This sample was sourced from the Wigunda Formation. In this sample six discrete age populations were observed (Figure 5D), the most significant population ca. 690-430 Ma zircons contained 18 (41.9%) of the <10% discordant grains. The next major population of 11 zircons (25.6%) had ages ranging from ca. 305-100 Ma. The remaining populations ca. 1150-840, 1490, 1770-1640 and 2015 Ma contained 10 (23.3%), 1 (2.3%), 2 (4.7%) and 1 (2.3%) zircon(s) respectively. The youngest <10% discordant  $U^{238}/Pb^{206}$  age is  $101.6\pm 1.7$  Ma (Lower Cretaceous, Albian) and is taken as the maximum depositional age.

GNARLYKNOTS-1A SAMPLE 74321 (DATA FROM MACDONALD ET AL. (2013B))

This sample was sourced from the Wigunda Formation. In this sample nine discrete age populations were observed (Figure 5E), the most significant population ca. 620-480 Ma zircons contained 18 (36%) of the <10% discordant grains. The next major population of 9 zircons (18%) had ages ranging from ca. 290-240 Ma. The remaining populations ca. 195-85, 803, 970-920, 1170-1100, 1645-1535, 2110-1860 and 2980-2960 Ma contained 8 (16%), 1 (2%), 3 (6%), 3 (6%), 3 (6%), 3 (6%) and 2 (4%) zircon(s) respectively. The youngest <10% discordant  $U^{238}/Pb^{206}$  age is  $85\pm 1.9$  Ma (Upper Cretaceous, Santonian) and is taken as the maximum depositional age.

GNARLYKNOTS-1A SAMPLE 74323 (DATA FROM MACDONALD ET AL. (2013B))

This sample was sourced from the Wigunda Formation. In this sample five age populations were observed (Figure 5G), the most significant population ca. 630-510 Ma zircons contained 32 (51.6%) of the <10% discordant grains. The next major population of 23 zircons (37.1%) had ages ranging from ca. 310-95 Ma. The remaining populations ca. 740-705, 1005-885 and 1360 Ma contained 3 (4.8%), 3 (4.8%) and 1 (1.6%) zircon(s) respectively. The youngest <10% discordant  $U^{238}/Pb^{206}$  age is  $95.1\pm 2.3$  Ma (Upper Cretaceous, Cenomanian) and is taken as the maximum depositional age.

GNARLYKNOTS-1A SAMPLE 74324 (DATA FROM MACDONALD ET AL. (2013B))

This sample was sourced from the Wigunda Formation. In this sample five age populations were observed (Figure 5H), the most significant population ca. 810-510 Ma zircons contained 34 (54.8%) of the <10% discordant grains. The next major population of 21 zircons (33.9%) had ages ranging from ca. 385-105 Ma. The remaining populations ca. 975-890, 1634 and 2000-1930 Ma contained 4 (6.5%), 1 (1.6%) and 2

(3.2%) zircon(s) respectively. The youngest <10% discordant  $U^{238}/Pb^{206}$  age is 105.4±5.6 Ma (Lower Cretaceous, Albian) and is taken as the maximum depositional age.

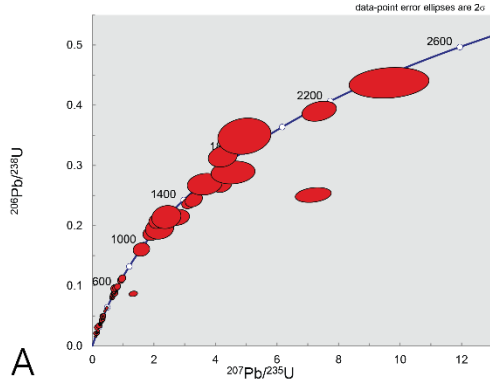
GNARLYKNOTS-1A SAMPLE 74325 (DATA FROM MACDONALD ET AL. (2013B))

This sample was sourced from the Wigunda Formation. In this sample six discrete age populations were observed (Figure 5I), the two most significant populations 335-235 Ma and 615-525 Ma each contained 12 (26.1%) of the <10% discordant grains. The next major population of 10 zircons (21.7%) had ages ranging from ca. 1280-820 Ma. The remaining two populations' ca. 430 and 2450-1690 Ma contained 1 (2.2%) and 5 (10.9%) zircon(s) respectively. The youngest <10% discordant  $U^{238}/Pb^{206}$  age is 99.3±3.1 Ma (Upper Cretaceous, Cenomanian) and is taken as the maximum depositional age.

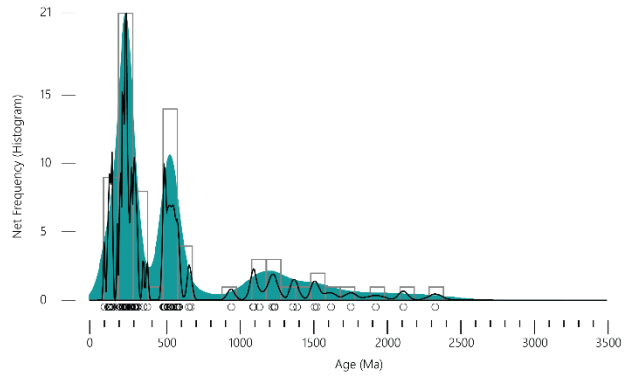
GNARLYKNOTS-1A SAMPLE 74326 (DATA FROM MACDONALD ET AL. (2013B))

This sample was sourced from the Wigunda Formation. In this sample six discrete age populations were observed (Figure 5J), the most significant population ca. 895-500 Ma zircons contained 29 (42.6%) of the <10% discordant grains. The next major population of 28 zircons (41.2%) had ages ranging from ca. 425-88 Ma. The remaining populations ca. 1260-1120, 1650-1595, 2070-1855 and 2705-2370 Ma contained 2 (2.9%), 3 (4.4%), 3 (4.4%) and 3 (4.4%) zircons respectively. The youngest <10% discordant  $U^{238}/Pb^{206}$  age is 88.2±4.5 Ma (Upper Cretaceous, Coniacian) and is taken as the maximum depositional age.

**Potoroo Formation, Gnarlyknots-1A Drill Hole, Sample 74317**

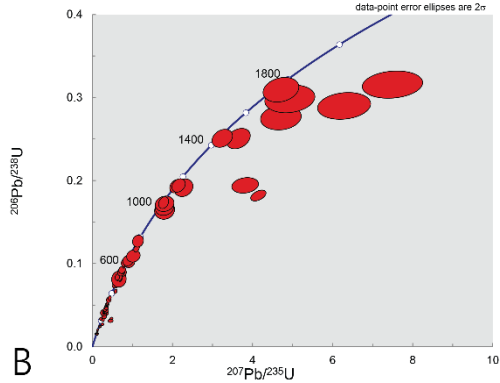


Gnarlyknots-1A, Sample 74317 (n=73)

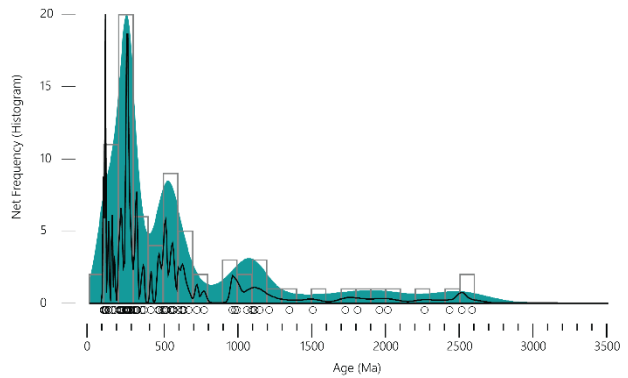


A

**Potoroo Formation, Gnarlyknots-1A Drill Hole, Sample 74318**

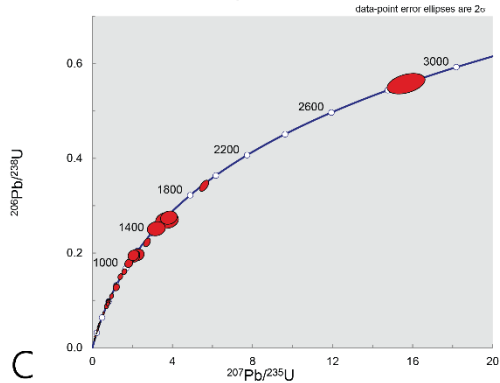


Gnarlyknots-1A, Sample 74318 (n=78)

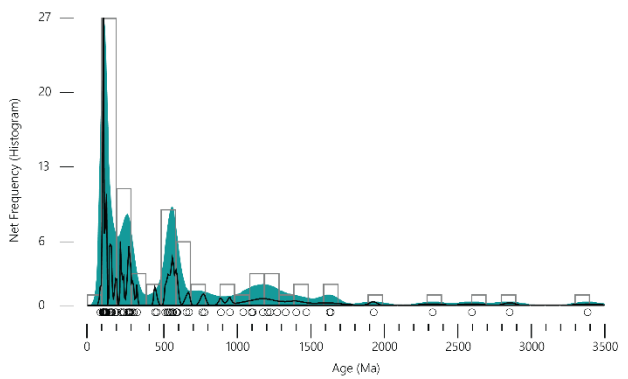


B

**Potoroo Formation, Gnarlyknots-1A Drill Hole, Sample 74319**

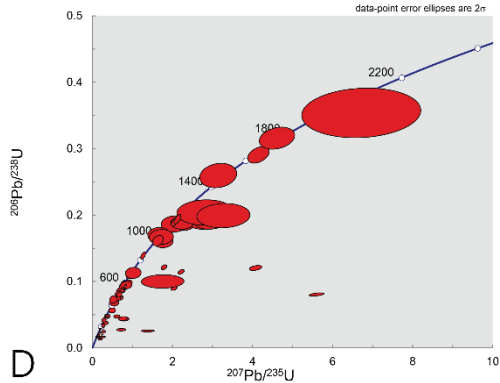


Gnarlyknots-1A, Sample 74319 (n=80)

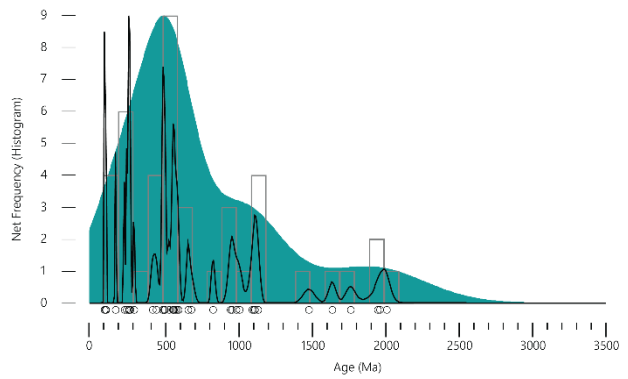


C

**Wigunda Formation, Gnarlyknots-1A Drill Hole, Sample 74320**

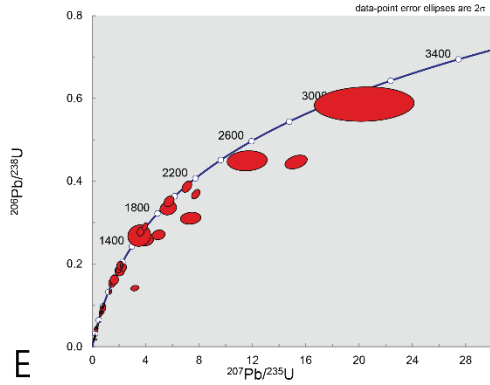


Gnarlyknots-1A, Sample 74320 (n=42)



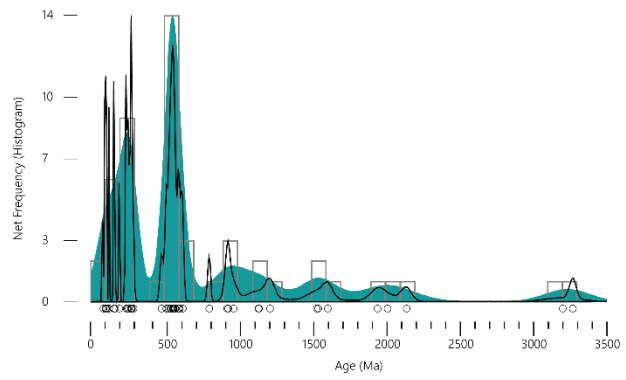
D

**Wigunda Formation, Gnarlyknots-1A Drill Hole, Sample 74321**

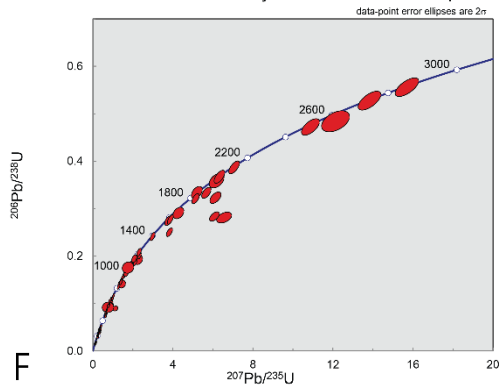


E

Gnarlyknots-1A, Sample 74321 (n=50)

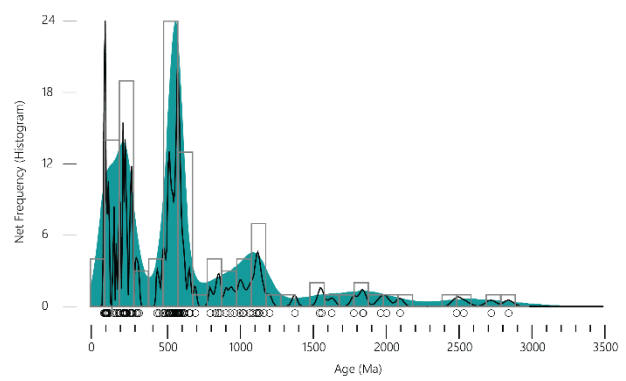


**Potoroo Formation, Gnarlyknots-1A Drill Hole, Sample 74322**

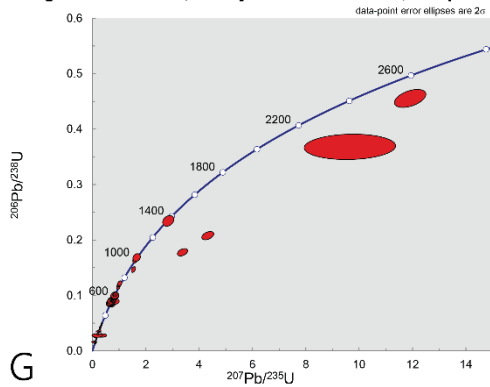


F

Gnarlyknots 1A Drill Hole, Sample 74322 (n=115)

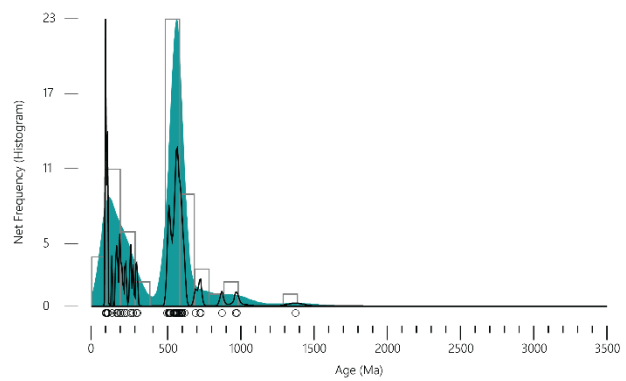


**Wigunda Formation, Gnarlyknots-1A Drill Hole, Sample 74323**

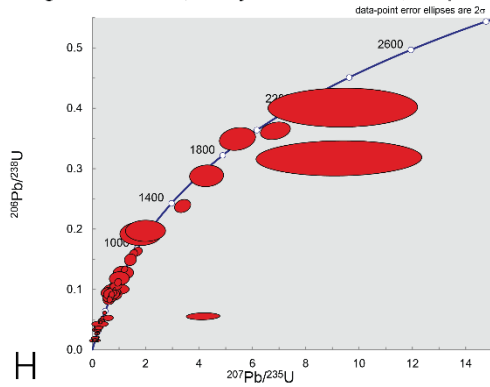


G

Gnarlyknots-1A, Sample 74323 (n=62)

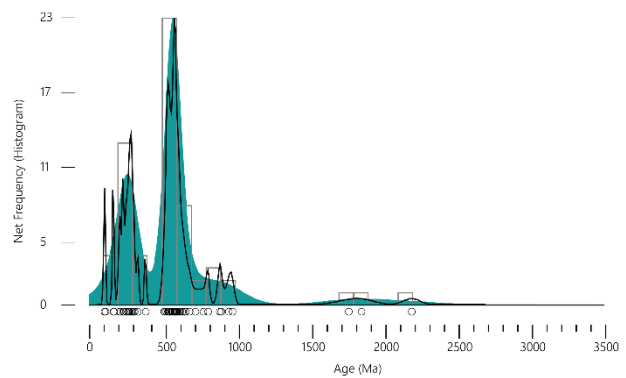


**Wigunda Formation, Gnarlyknots-1A Drill Hole, Sample 74324**



H

Gnarlyknots-1A, Sample 74324 (n=62)





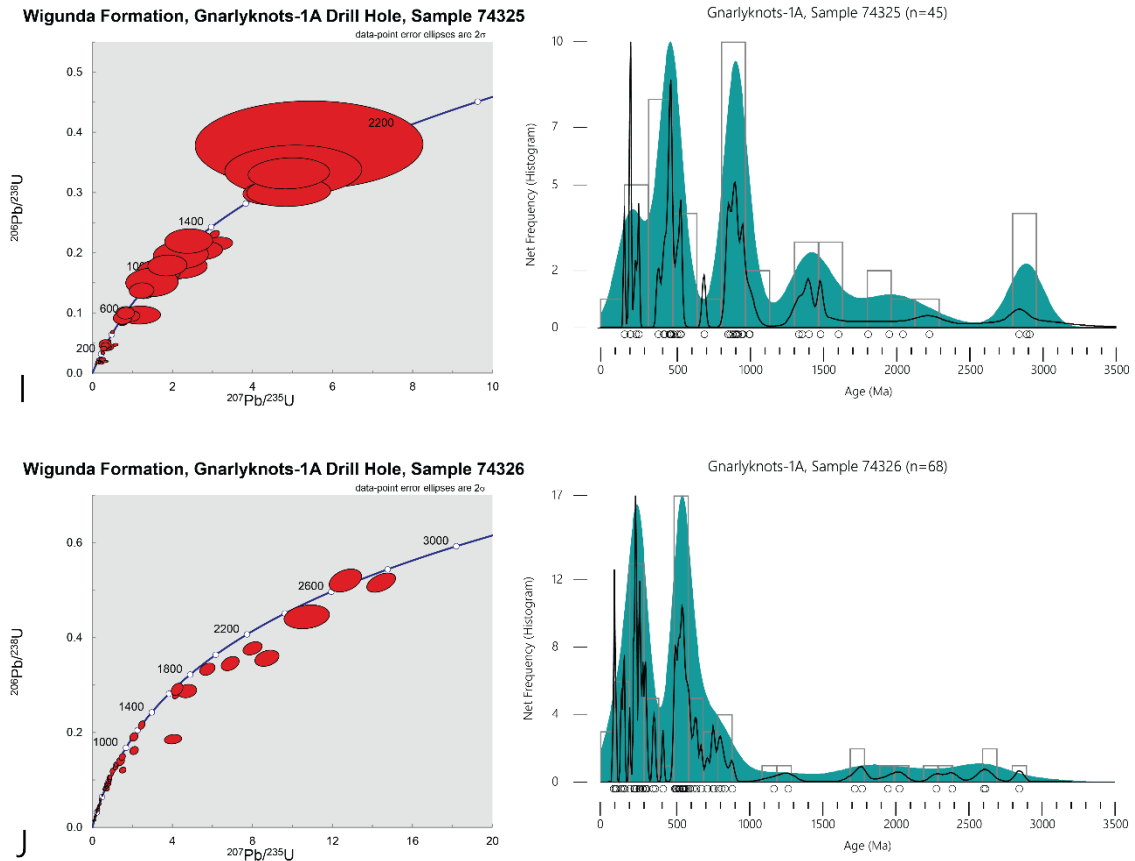


Figure 5A-J: Uranium-lead Concordia plots showing all data for each Gnarlyknots-1A sample with corresponding kernel density estimate (green shading, adaptive bandwidth), probability density plot (black line) and histogram (grey boxes, net frequency on Y-axis, 100 Ma bin width) using 90-110 concordant data with each datum represented by a black circle on the X-axis.

#### WINTON FORMATION SAMPLES 8622-61 AND 8642-168 (DATA FROM MACDONALD AND HOLFORD PERS. COMM. 2014)

These two samples are sourced from the Winton Formation in western Eromanga basin drill holes, Burley-2 and Dullingari-1.

There were six discrete age populations in sample 8622-61 (Figure 6A). The most significant population ca. 570-205 Ma zircons contained 45 (62.5%) of the <10% discordant grains. The other major population of 12 (16.7%) grains had ages ranging from ca. 2055-1560 Ma. The remaining populations ca. 170-120, 930-790, 1370-1200 and 2700-2300 Ma contained 5 (6.9%), 4 (5.6%), 2 (2.8%) and 4 (5.6%) zircons

respectively. The youngest <10% discordant  $U^{238}/Pb^{206}$  grain is  $120.3 \pm 1.8$  Ma (Lower Cretaceous, Aptian) and is taken as the maximum depositional age.

In sample 8642-168, six discrete age populations were identified (Figure 6B). The most significant population ca. 125-90 Ma zircons contained 14 (29.2%) of the <10% discordant grains. The next major population of 13 (27.1%) grains had ages ranging from ca. 700-410 Ma. The remaining populations ca. 380-180, 1260-890, 1611 and 2840 Ma contained 12 (25%), 7 (14.6%), 1 (2.1%) and 1 (2.1%) zircon(s) respectively. The youngest <10% discordant  $U^{238}/Pb^{206}$  grain is  $94.2 \pm 1.7$  Ma (Upper Cretaceous, Cenomanian) and is taken as the maximum depositional age.

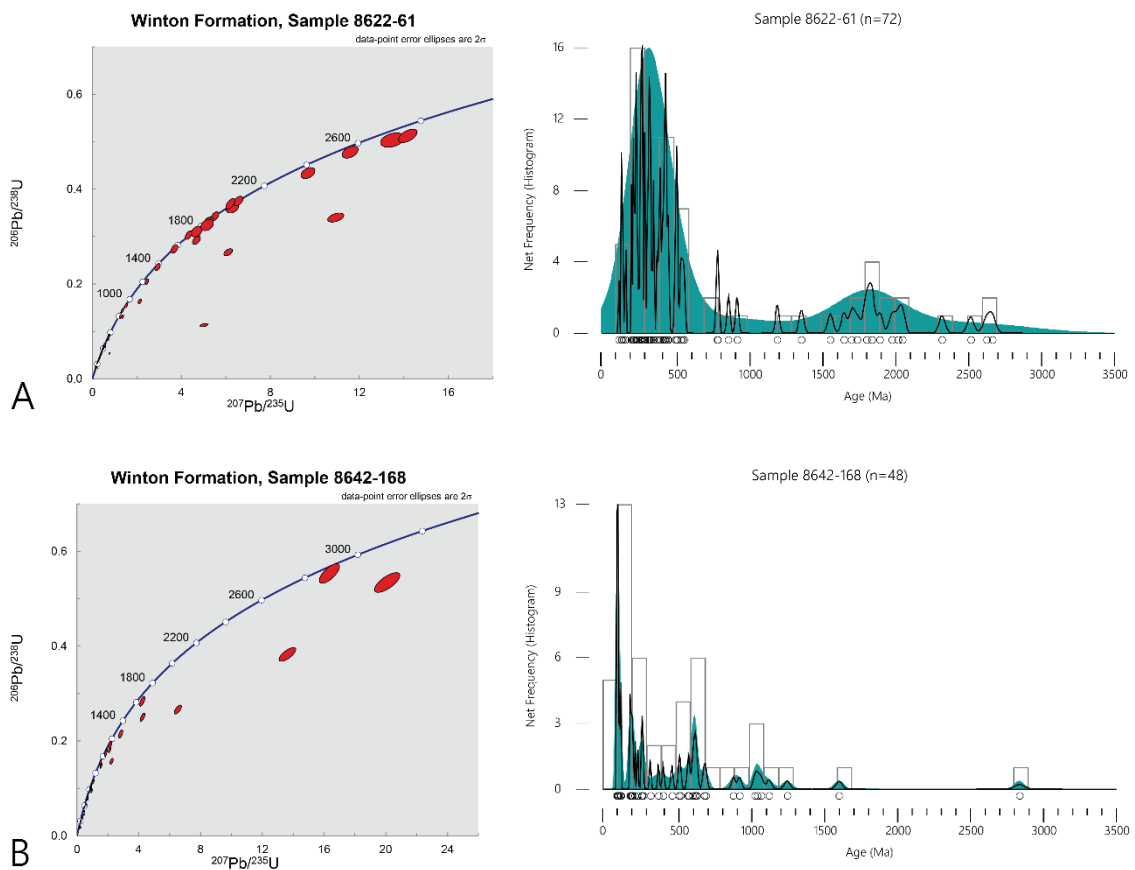


Figure 6A&B: Uranium-lead Concordia plots showing all data for two western Eromanga basin samples from Dullingari-1 and Burely-2 drill holes with corresponding kernel density estimate (green shading, adaptive bandwidth), probability density plot (black line) and histogram (grey boxes, net frequency on Y-axis, 100 Ma bin width) using 90-110 concordant data with each datum represented by a black circle on the X-axis.

EROMANGA-1 (DATA FROM TUCKER ET AL. (2013))

This sample was sourced from the Winton Formation. In the sample seven discrete populations were observed (Figure 7A), the most significant population ca. 170-93 Ma zircons contained 65 (69.1%) of the <10% discordant grains. The next major population of 9 zircons (9.6%) had ages ranging from ca. 2055-1560 Ma. The remaining populations ca. 345-245, 650-500, 1030-830, 1680-1560 and 3340-3050 Ma contained 8 (8.5%), 4 (4.3%), 4 (8.3%), 2 (2.1%) and 2 (2.1%) zircons respectively. The youngest <10% discordant  $U^{238}/Pb^{206}$  grain is  $93.0 \pm 1.1$  Ma (Upper Cretaceous, Turonian) and is taken as the maximum depositional age.

ISISFORD (DATA FROM TUCKER ET AL. (2013))

This sample was sourced from the Winton Formation. In the sample five discrete populations were observed (Figure 7B), the most significant population ca. 125-100 Ma zircons contained 23 (37.7%) of the <10% discordant grains. The next major population of 21 zircons (34.4%) had ages ranging from ca. 295-155 Ma. The remaining populations ca. 720-370, 1210-950 and 3260-2670 Ma contained 8 (13.1%), 5 (8.2%) and 4 (6.6%) zircons respectively. The youngest <10% discordant  $U^{238}/Pb^{206}$  grain is  $100.5 \pm 1.1$  Ma (Upper to Lower Cretaceous, Cenomanian to Albian) and is taken as the maximum depositional age.

LARK QUARRY CONSERVATION PARK (DATA FROM TUCKER ET AL. (2013))

This sample was sourced from the Winton Formation. In the sample five discrete populations were observed (Figure 7C), the most significant population ca 310-95 Ma zircons contained 36 (70.6%) of the <10% discordant grains. The next major population of 10 zircons (19.6%) had ages ranging from ca. 595-530 Ma. The remaining

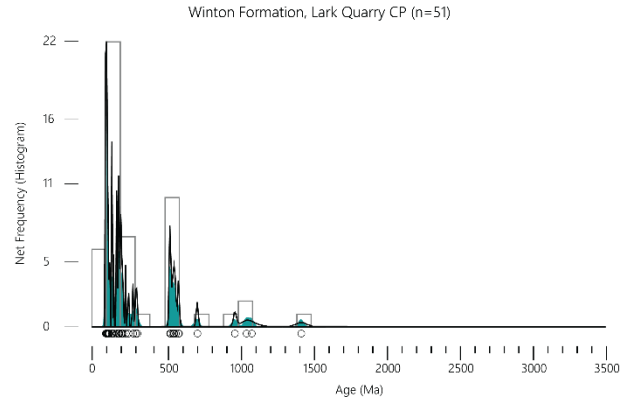
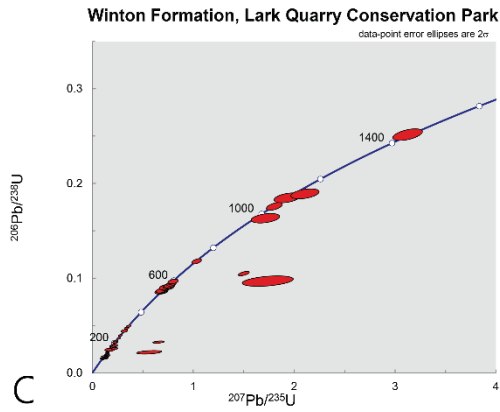
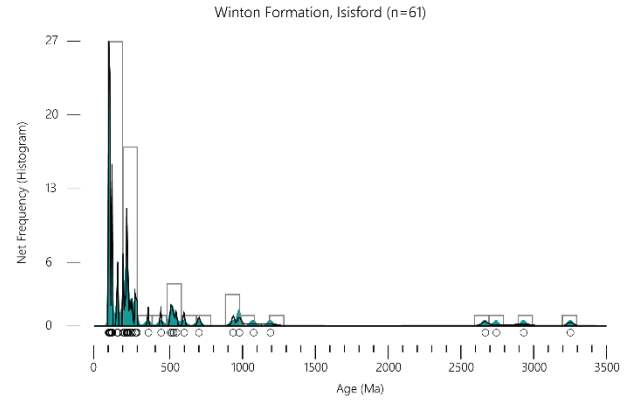
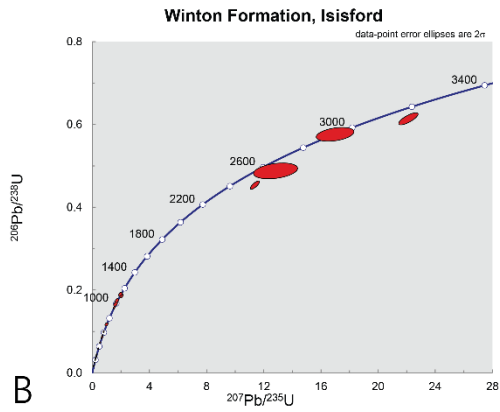
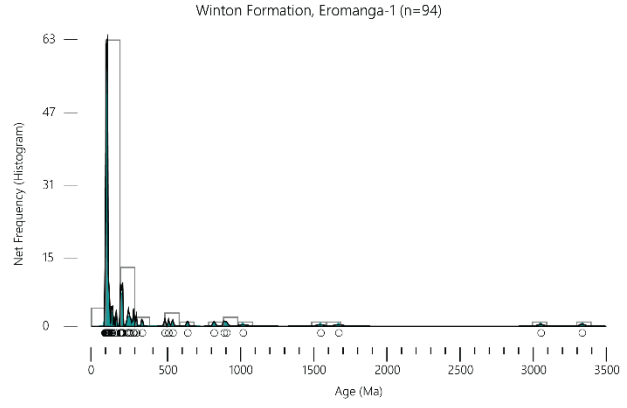
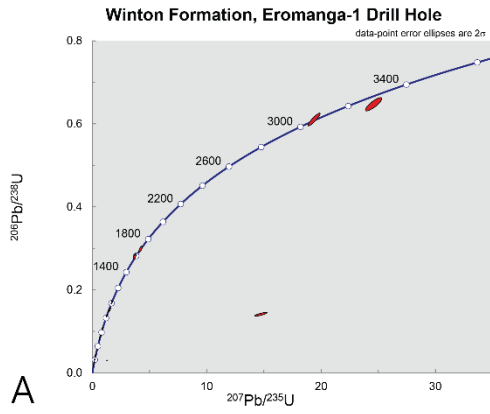
populations ca. 720, 1090-975 and 1430 Ma contained 1 (2%), 3 (5.9%) and 1 (2%) zircon(s) respectively. The youngest <10% discordant U238/Pb206 grain is  $96.7 \pm 1.3$  Ma (Upper Cretaceous, Cenomanian) and is taken as the maximum depositional age.

#### BLADENSBURG NATIONAL PARK (DATA FROM TUCKER ET AL. (2013))

This sample was sourced from the Winton Formation. In the sample seven discrete populations were observed (Figure 7D), the most significant population ca. 280-93 Ma zircons contained 51 (66.2%) of the <10% discordant grains. The next major population of 12 zircons (15.6%) had ages ranging from ca. 720-515 Ma. The remaining populations ca. 360-340, 1120-850, 1850-1710, 2500 and 3280 Ma contained 2 (2.6%), 8 (10.4%), 2 (2.6%), 1 (1.3%) and 1 (1.3%) zircon(s) respectively. The youngest <10% discordant U238/Pb206 grain is  $93.3 \pm 1.2$  Ma (Upper Cretaceous, Turonian) and is taken as the maximum depositional age.

#### LONGREACH-1 (DATA FROM TUCKER ET AL. (2013))

This sample was sourced from the Mackunda Formation. In the sample eight discrete populations were observed (Figure 7E), the most significant population ca. 290-100 Ma zircons contained 43 (64.2%) of the <10% discordant grains. The next major population of 15 zircons (22.4%) had ages ranging from ca. 730-340 Ma. The remaining populations ca. 890, 1210-1040, 1430, 2260, 2720-2650 and 3060 Ma contained 1 (1.5%), 3 (4.5%), 2 (3.0%), 1 (1.5%), 1 (1.5%) and 1 (1.5%) zircon(s) respectively. The youngest <10% discordant U238/Pb206 grain is  $102.5 \pm 1.3$  Ma (Lower Cretaceous, Albian) and is taken as the maximum depositional age.



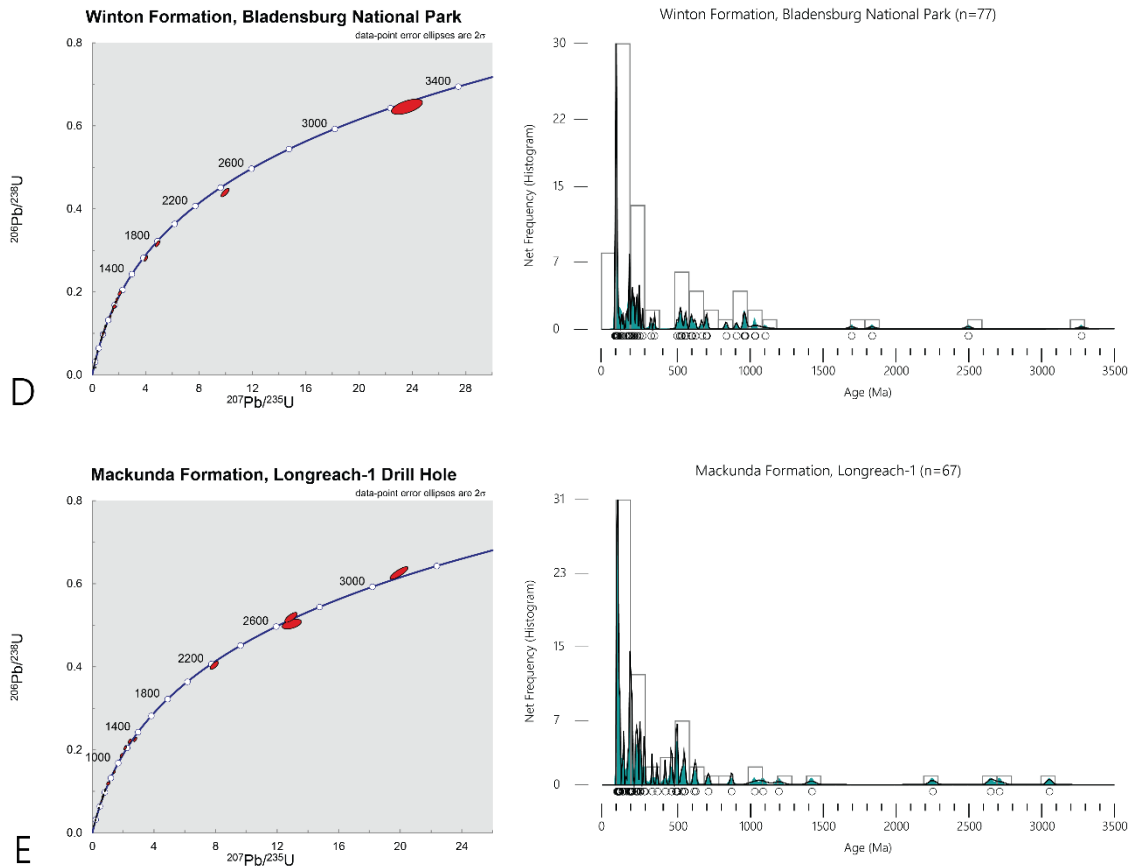


Figure 7A-E: Uranium-lead Concordia plots showing all data for five central and eastern Eromanga basin samples with corresponding kernel density estimate (green shading, adaptive bandwidth), probability density plot (black line) and histogram (grey boxes, net frequency on Y-axis, 100 Ma bin width) using 90-110 concordant data with each datum represented by a black circle on the X-axis.

HUGHES-2 SAMPLE 1069106 (DATA FROM MACDONALD AND HOLFORD PERS. COMM. 2014)

This sample was sourced from the Loongana Formation of the Bight Basin, age of formation, Valanginian to Hauterivian (Hill 1991), so significantly older than the previous samples. In this dataset two discrete populations were observed (Figure 8A), the most significant population ca. 1310-1075 Ma zircons contained 55 (90.2%) of the <10% discordant grains. The other population of 6 zircons (9.8%) had ages ranging from ca. 1755-1540 Ma. The youngest <10% discordant  $\text{U}^{238}/\text{Pb}^{206}$  age is  $1076.4 \pm 21.4$  Ma (Mesoproterozoic, Stenian) and is taken as the maximum depositional age. This is significantly older than the depositional age of the formation.

HUGHES-2 SAMPLE 1069111 (DATA FROM MACDONALD AND HOLFORD PERS. COMM. 2014)

This sample was also sourced from the Valanginian to Hauterivian Loongana Formation (Hill 1991). In the dataset three discrete populations were observed (Figure 8B), the most significant population ca. 1330-1025 Ma zircons contained 43 (62.3%) of the <10% discordant grains. The other major population of 25 zircons (62.3%) had ages ranging from ca. 1800-1425 Ma. The final population contained only one <10% discordant grain aged  $681 \pm 12.6$  Ma (Neoproterozoic, Cryogenian). This was also the youngest <10% discordant  $U^{238}/Pb^{206}$  age and is taken as the maximum depositional age. This is still significantly older than the age of formation.

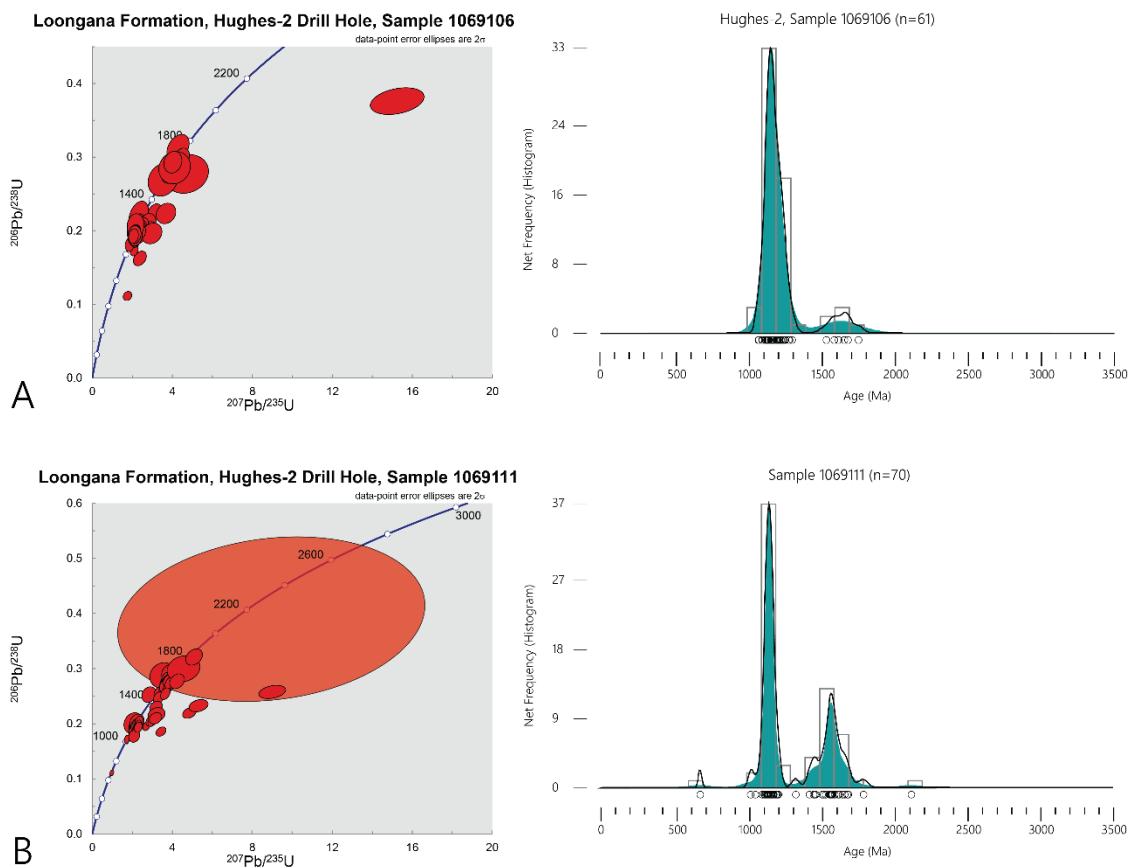


Figure 8A&B: Uranium-lead Concordia plots showing all data for Hughes-2 drill hole samples 109106 and 1069111 with corresponding kernel density estimate (green shading, adaptive bandwidth), probability density plot (black line) and histogram (grey boxes, net frequency on Y-axis, 100 Ma bin width) using 90-110 concordant data with each datum represented by a black circle on the X-axis.

## New U-Pb Data

### GNARLYKNOTS-1A SAMPLE 74322

Additional data were collected from Gnarlyknots-1A sample 74322 to expand the U-Pb and hafnium datasets for Gnarlyknots-1A. This particular sample was deemed most suitable for this purpose as the images were of higher quality than any other Gnarlyknots-1A sample. A further 55 U-Pb data were acquired with 53 of these being  $\pm 10\%$  concordant (Figure 9A). These data were added to the existing U-Pb dataset (Figure 9B) from MacDonald et al. (2013b) for Gnarlyknots-1A sample 74322 (Figure 5F). This sample was sourced from the Turonian to Santonian Wigunda Formation. Using the complete dataset for sample 74322, six discrete age populations were identified (Figure 5F). The most significant population ca. 715-455 Ma zircons contained 42 (35.9%) of the <10% discordant grains. The next major population of 40 zircons (34.2%) had ages ranging from ca. 330-90 Ma. The remaining populations ca. 1220-815, 1650-1395, 2110-1795 and 2850-2495 Ma contained 20 (17.1%), 4 (3.4%), 7 (6.0%) and 4 (3.4%) zircons respectively. The youngest <10% discordant  $U^{238}/Pb^{206}$  age is  $91.3 \pm 3.2$  Ma (Upper Cretaceous, Turonian) and is taken as the maximum depositional age.



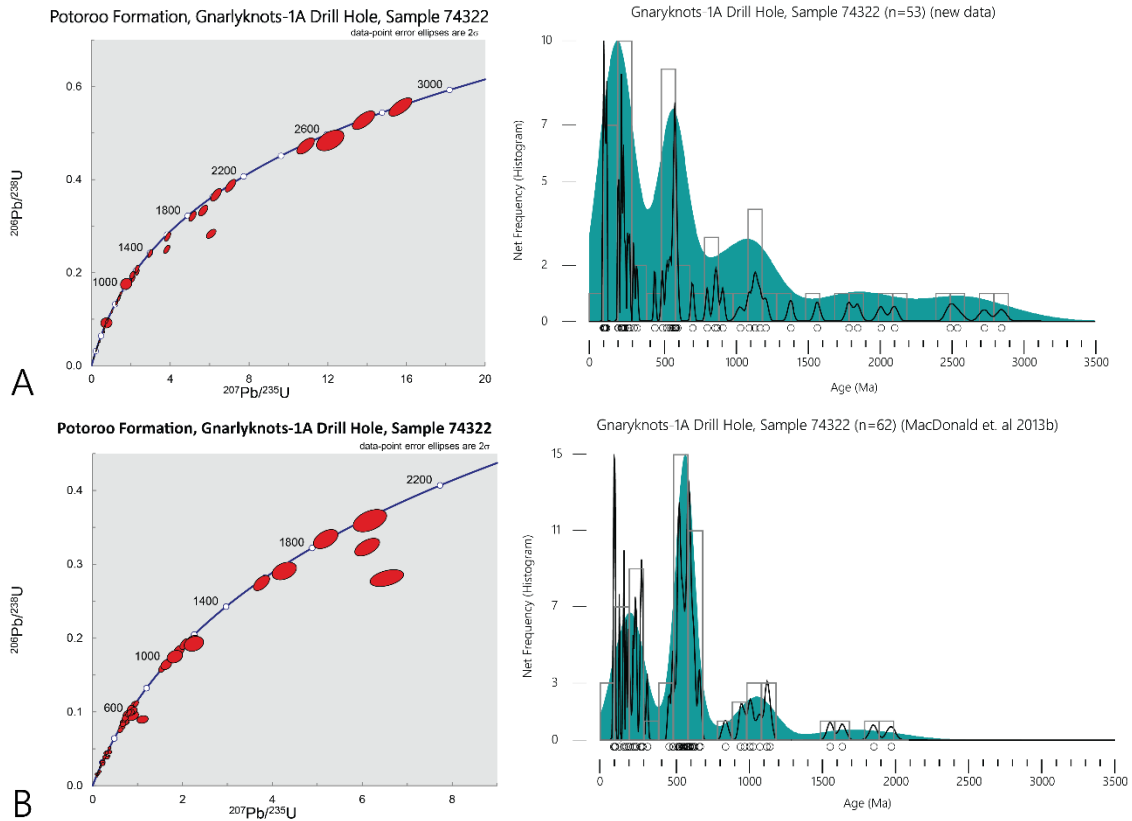


**Figure 9A&B: Uranium-lead Concordia plots showing new uranium-lead data (A) and previous data from MacDonald et al. (2013b) (B) for Gnarlyknots-1A sample 74322 with corresponding kernel density estimate (green shading, adaptive bandwidth), probability density plot (black line) and histogram (grey boxes, net frequency on Y-axis, 100 Ma bin width) using 90-110 concordant data with each datum represented by a black circle on the X-axis.**

### HUGHES-2 SAMPLE 106988

A total of 62 U-Pb data were acquired from the Hughes-2 sample 106988, with 58 of these being  $\pm 10\%$  concordant. The youngest  $< 10\%$  discordant  $\text{U}^{238}/\text{Pb}^{206}$  age is  $1048.9 \pm 15.2$  Ma (Mesoproterozoic, Stenian) and is taken as the maximum depositional age. Two distinct populations of zircons, shown in Figure 10, are present in the sample. The major population comprising 47 (81%) of  $\pm 10\%$  concordant zircons ranges in ages ca. 1330-1040 Ma. The second population, comprising of 11 (19%) of  $\pm 10\%$  concordant zircons ranges in ages ca. 1780-1500 Ma. These Mesoproterozoic to Paleoproterozoic zircons are significantly older than the Valanginian to Hauterivian age of the Loongana formation, (Hill 1991), from where this sample was sourced.

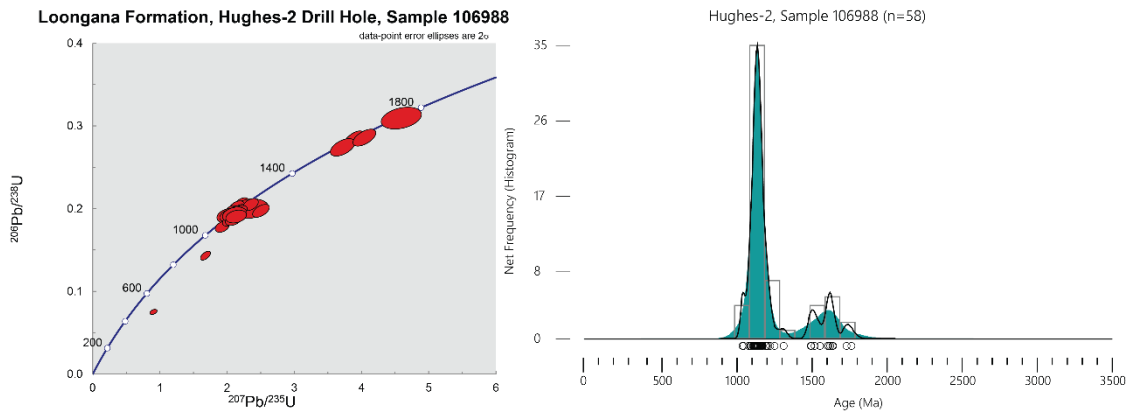


Figure 10: Uranium-lead Concordia plots showing all data for Hughes-2 sample 106988 with corresponding kernel density estimate (green shading, adaptive bandwidth), probability density plot (black line) and histogram (grey boxes, net frequency on Y-axis, 100 Ma bin width) using 90-110 concordant data with each datum represented by a black circle on the X-axis.

### Gnarlyknots-1A Hafnium Analyses

Corrected  $\epsilon\text{Hf}$  values from Gnarlyknots-1A are given in Figure 11, isotope ratios were taken from samples 74318, 74319, 74321, 74322, 74323 and 74326. There were large variances in age corrected  $\epsilon\text{Hf}$  values ranging from highly evolved (-46.4) to very juvenile (+19.9). There are distinct and diffuse populations in the dataset that correspond to the uranium-lead age populations, and in a number of cases, distinguish between similar-aged populations.

With one exception, all 3000-2300 Ma zircons show negative  $\epsilon\text{Hf}$  values indicating an evolved source for those zircons. One zircon in this age, ~2859 Ma, shows a highly positive  $\epsilon\text{Hf}$  value, indicating a juvenile source. There is a general trend of less negative values with increasing age in this population. Epsilon Hf values range from -19.6 to +9.1.

A second population ca. 2000-1400 Ma shows a general trend of increasingly negative values corresponding with increasing age. Epsilon Hf values range from juvenile (+7.4) to evolved (-8.4).

Late Mesoproterozoic zircons (ca. 1260-1080 Ma) show two subpopulations. One population at ca. 1100 Ma includes zircons with moderately evolved  $\epsilon\text{Hf}$  values (-6.7 to

-5.0). The second coeval population is characterised by  $\epsilon\text{Hf}$  values spanning zero (-1.5 to +1.9). This may indicate two different zircon sources. One zircon (~1139 Ma) has an  $\epsilon\text{Hf}$  value of +11.7 indicating a highly juvenile source.

Zircons spanning the Mesoproterozoic-Neoproterozoic boundary, between ca. 1030-895 Ma, show generally positive  $\epsilon\text{Hf}$  values, indicating a juvenile source; however, there are two evolved zircons. Epsilon Hf values range from -9.6 to +19.7 although most values lie between -1.8 and +9.3.

There is a large Neoproterozoic to Palaeozoic population between ca. 800-450 Ma.

These involve 60 analyses and make up 40% of the analysed zircons. The older zircons in this population (ca. 800-650 Ma) span the zero  $\epsilon\text{Hf}$  line, broadly between +5 and -3.

After ~650 and until ~455 Ma many zircons show a vertical spread between ca. +2.1 and highly evolved values down to -17.5. There is also a smaller population ca. 570-513 Ma with highly negative (-28 to -23.3).

Silurian and Devonian zircons are absent, but Carboniferous to Lower Jurassic zircons (ca. 360-180 Ma) form two distinct  $\epsilon\text{Hf}$  populations. An evolved population ( $\epsilon\text{Hf}$  -13.3 to -3) occurs with ca. 360-180 Ma zircons. A second population overlapping in age (ca. 320-200 Ma), but generally younger than the previous population, has moderately juvenile  $\epsilon\text{Hf}$  values range from -0.6 to +8.5 with most falling between +3 and +8.5.

A final population of Lower Jurassic to Cretaceous zircons (ca. 180-95 Ma) contains moderate to highly juvenile  $\epsilon\text{Hf}$  values (+4.3 to +12.8). Within this population a tight grouping (approx. 74%) of juvenile zircons occur between ~130 Ma and ~95 Ma.

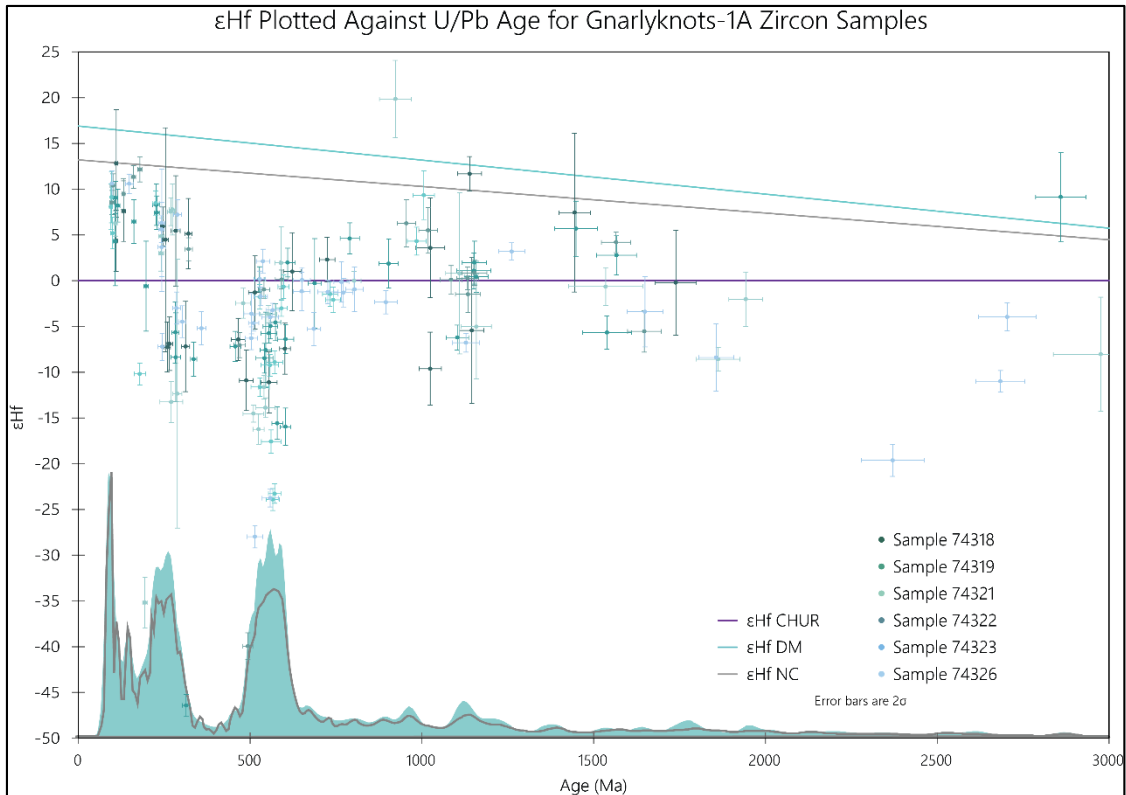


**Figure 11: Plot showing epsilon hafnium in relation to uranium-lead age of Gnarlyknots-1A zircon samples. A chondritic uniform reservoir reference line (purple) plots along (x, 0), the epsilon hafnium depleted mantle line (aqua) shows the modelled mantle epsilon hafnium values and the epsilon hafnium new crust line (grey) shows the new epsilon hafnium mantle model values as suggested by Dhuime et al. (2011). The epsilon hafnium values provide information about the material that melted to form the magma from which the zircon crystallised. Negative epsilon hafnium values indicate involvement of existing continental crust in magma genesis; conversely positive epsilon hafnium values indicate the source had experienced a prior depletion event. Data points below the chondritic uniform reservoir are considered evolved, above the depleted mantle are highly depleted and between the chondritic uniform reservoir and depleted mantle are considered juvenile. The kernel density estimate (green shaded area) and probability density plot (black solid line) are overlain for visual correlation of zircon populations.**

## DISCUSSION

### Maximum Depositional Ages

The oldest sedimentary rocks analysed were from the Lower Cretaceous Loongana Formation (ca. 139-129 Ma) in the Hughes-2 core. Two of the three Hughes-2 samples, 1069106 and 106988, had Stenian maximum depositional ages,  $1076 \pm 21$  and  $1049 \pm 15$  Ma respectively. The final Hughes-2 sample, 1069111 had a Cryogenian maximum depositional age of  $681 \pm 13$  Ma. These are significantly older than any other analysed

sample maximum depositional ages, and much older than the actual depositional age.

These are shown in Figure 12A.

The next oldest sample, which borders the Upper and Lower Cretaceous boundary (ca. 100-97 Ma), was the Mackunda Formation from the Longreach-1 core. The maximum depositional age of this sample was  $102.5 \pm 1.3$  Ma (Figure 12B).

Samples from the stratigraphically younger and overlying (see Figure 4) Turonian to late Albian (ca 7-90 Ma) Winton Formation were the next oldest. The two western Eromanga samples had maximum depositional ages of  $120.3 \pm 1.8$  and  $94.2 \pm 1.7$  Ma. The eastern samples (Tucker et al. 2013) had maximum depositional ages of  $100.5 \pm 1.1$ ,  $96.7 \pm 1.3$ ,  $93.3 \pm 1.2$  and  $93.0 \pm 1.1$  for samples Isisford, Lark Quarry Conservation Park, Bladensburg National Park and Eromanga-1 respectively. These are shown in Figure 12B.

The youngest formations, the Wigunda and Potoroo Formations from Gnarlyknots-1A have relatively consistent depositional ages, particularly when considering their two sigma errors. There is a very slight trend of decreasing maximum depositional age with increasing depth (as shown in Figure 12D); however, this trend is not well defined and further, accurate sampling is necessary to confirm or deny this trend. The maximum depositional ages from the stratigraphically oldest sample to the youngest are  $88.2 \pm 4.5$ ,  $99.3 \pm 3.1$ ,  $105.4 \pm 5.6$ ,  $95.1 \pm 2.3$ ,  $91.3 \pm 3.2$ ,  $85 \pm 1.9$ ,  $101.6 \pm 1.7$ ,  $100.6 \pm 2.4$ ,  $98.9 \pm 2$  and  $103.5 \pm 4.7$  Ma for Gnarlyknots-1A samples 74326, 74325, 74324, 74323, 74322, 74321, 74320, 74319, 74318 and 74317 respectively. These are shown in Figure 12C.

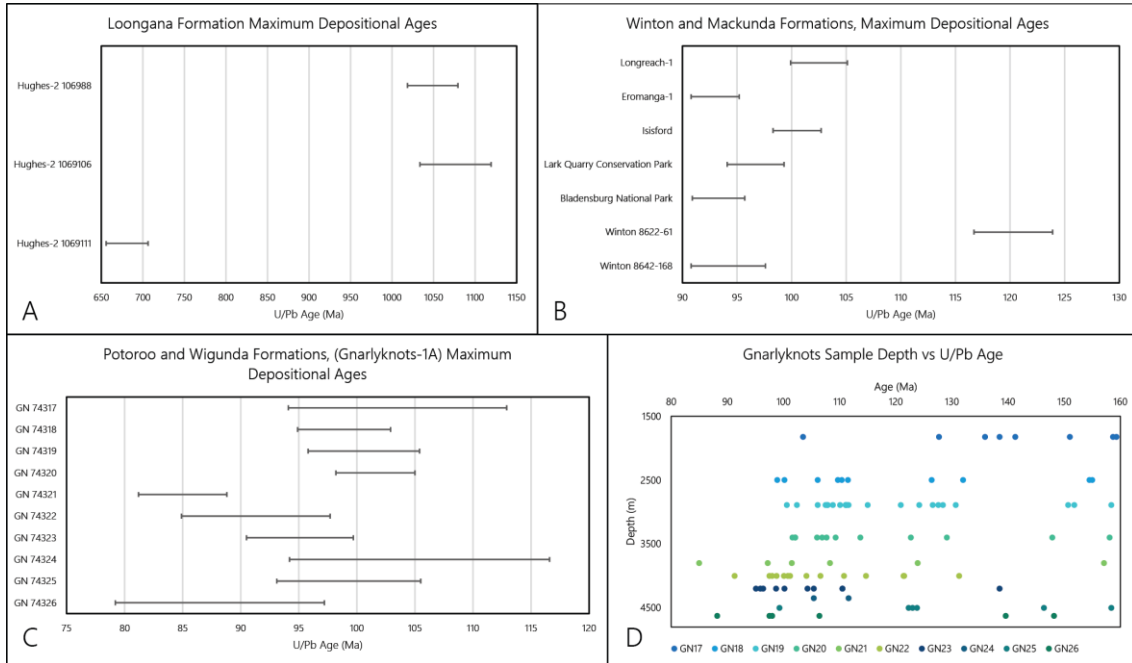


**Figure 12 A-D:** Maximum depositional ages determined by the youngest near concordant  $U^{238}/Pb^{206}$  age errors plotted at the  $2\sigma$  level, for: (A) Mackunda Formation (Longreach-1), and Winton Formation, (B) Loongana Formation from Hughes-2 and (C) Potoroo Formation (GN 74317-74319) and Wigunda Formation (GN 74320-74326). A slight trend of decreasing age (using only <160 Ma, <10% discordant zircons) with increasing sample depth for the Gnarlyknots-1A samples is shown in (D). This suggests progressive erosion of a normally layered sedimentary succession.

## U-Pb Age Provenance of the Cretaceous in South Australia

The detrital zircon age spectra of all three Loongana Formation samples from Hughes-2 are essentially identical (Figure 8 and Figure 10). With the exception of sample 1069111 having a small peak at ~680 Ma, two peaks are present in each sample, a major, acute peak between ~1200 and ~1100 Ma, and a second broad peak between

~1700 and ~1400 Ma. Figure 13 is a composite plot showing all near concordant data for the Loongana Formation samples.

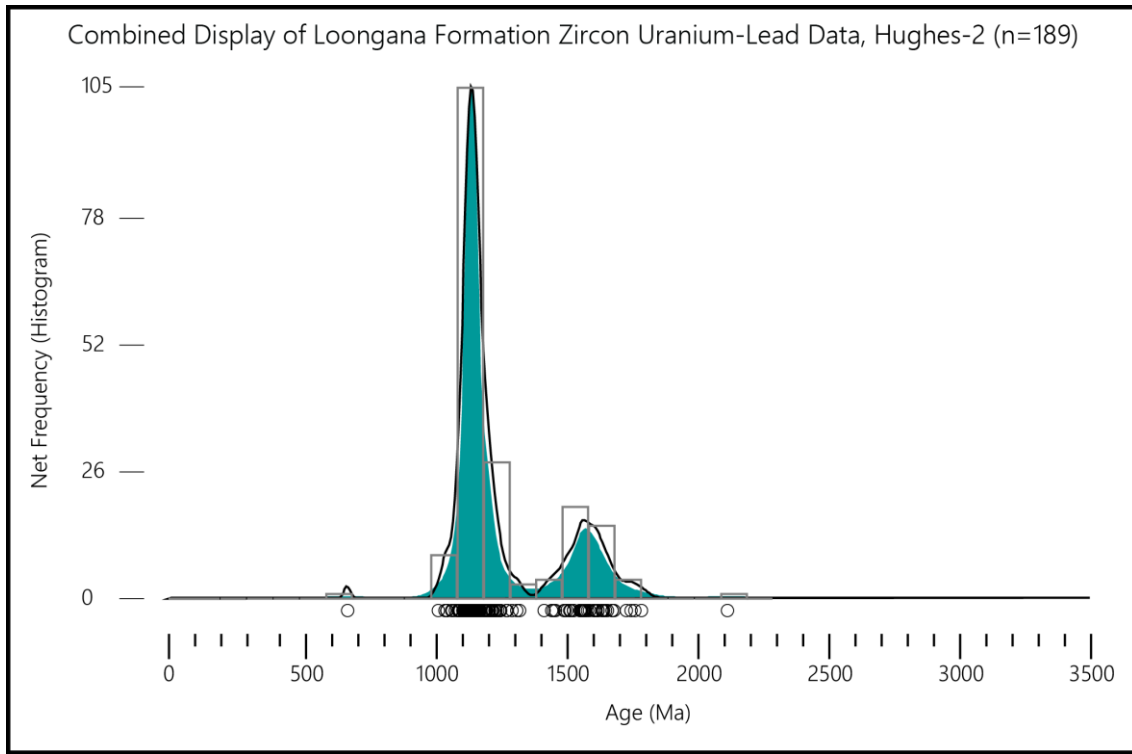


Figure 13: Combined display of zircon uranium-lead ages for Hughes-2, Bight Basin, showing histogram (grey rectangles, net frequency shown on Y-axis, bin-width of 100), kernel density estimate (green shading, adaptive bandwidth) and probability distribution plot (black line). Each datum is represented by a black circle on the X-axis.

The ca. 1700-1400 Ma zircons may be sourced from the Mount Painter Province. Data from Kromkhun et al. (2013) shows the same bimodal peak for igneous intrusions of the Mount Painter Province. These may also be sourced from the Musgrave Province as the ages are similar to those presented by Wade et al. (2006). Future hafnium analysis on the Hughes-2 samples will aid an accurate determination of source region. The ca. 1200-1100 Ma population is likely sourced from the Musgrave Province with an age population similar to that presented by Smithies et al. (2011).

The provenance of the Winton (and Mackunda) Formation has been recently investigated in detail by Tucker (2014). The results obtained in this study agree with their findings. Almost all of the Winton Formation age spectra are essentially identical

and are thus collectively described with the exception of Winton 8622-61 which shows a more similar spectra to that of the Mackunda Formation presented by Tucker (2014).

Figure 14 is a composite plot of all Winton Formation samples, excluding Winton 8622-61.

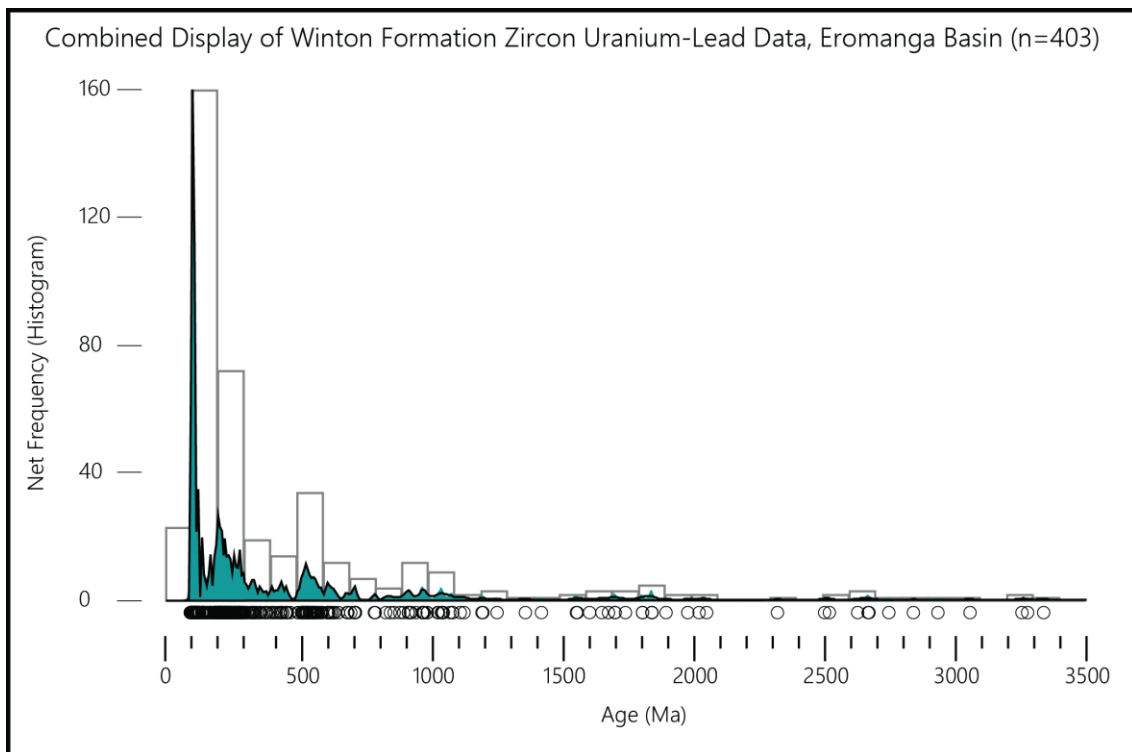


**Figure 14:** Combined display of zircon uranium-lead ages for Winton Formation samples, showing histogram (grey rectangles, net frequency shown on Y-axis, bin-width of 100), kernel density estimate (green shading, adaptive bandwidth) and probability distribution plot (black line). Each datum is represented by a black circle on the X-axis

Few Archean zircons are present, which fits with the limited Archean in NE Australia. It is plausible that these zircons are sourced from the west and southwestern Archean terranes including the Gawler Craton. The Proterozoic populations are generally small, with concentrations around ca. 2000-1500 Ma and 1200-800 Ma. These Proterozoic grains are likely to have several sources including the Musgrave Province, the Georgetown and Mount Isa Inliers. Paleozoic zircons are significantly more abundant than both Archean and Proterozoic zircons. Population density generally increases toward the Permian, with a significant peak during the Late Cambrian while Ordovician



to Silurian grains are less abundant. The Cambrian to Devonian grains are likely sourced locally from areas including the Charters Towers Province, Anakie Province and the Macrossan and Pama Igneous bodies. Carboniferous to Permian zircons become more prevalent and are plausibly sourced from the New England Fold Belt and Kennedy Igneous Province (Bryan et al. 2004). Mesozoic zircons are the most populous in the Winton Formation with Cretaceous grains being more abundant than the Triassic and Jurassic zircons. Tucker (2014) stated that there is no known source terrane within Queensland or eastern Australia for the Jurassic and Late Triassic populations; however, Li et al. (2012) demonstrated granite crystallisation ages down to ca. 217 Ma in the region. The Cretaceous zircons are interpreted to be sourced from the Whitsunday Volcanic Province (Bryan et al. 2000, Bryan et al. 2012, Tucker 2014). Regardless of stratigraphic age and sample depth, all ten samples from Gnarlyknots-1A show no discernible differences in age spectra and can be considered similar, thus a composite plot (Figure 15) showing all concordant Gnarlyknots-1A is suitable for provenance analysis.

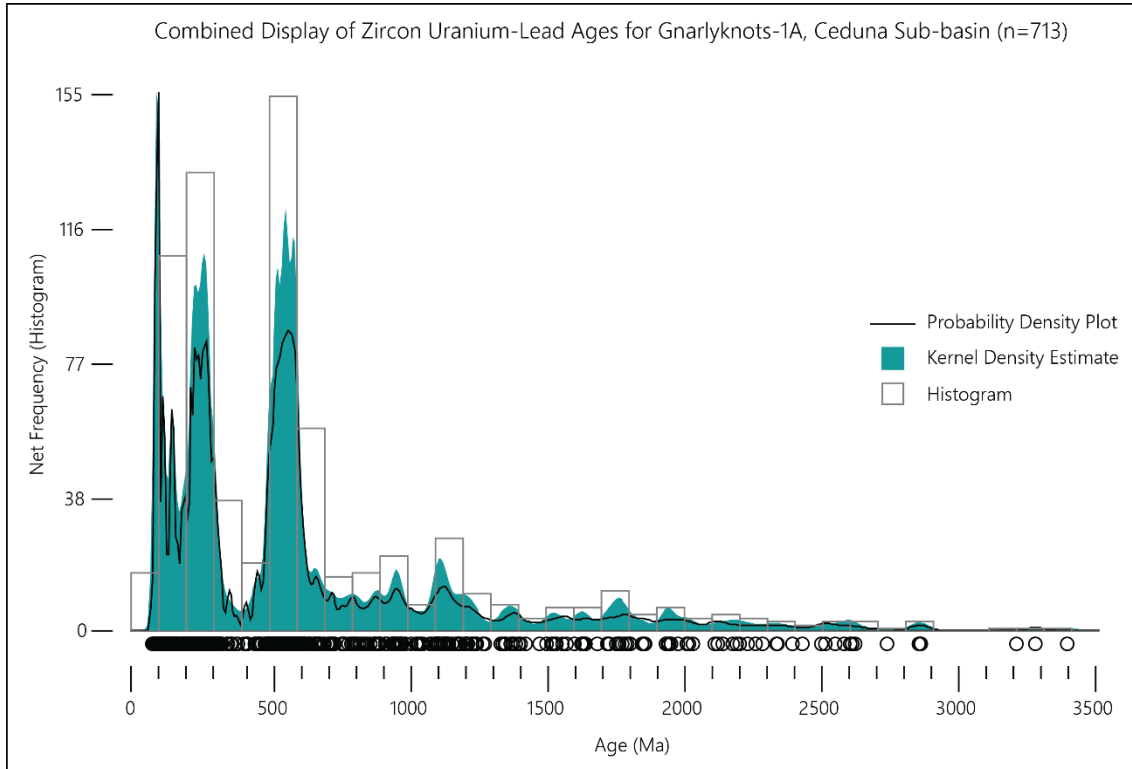


Figure 15: Combined display of zircon uranium-lead ages for Gnarlyknots-1A, Ceduna Sub-basin, showing histogram (grey rectangles, net frequency shown on Y-axis, bin-width of 100), kernel density estimate (green shading, adaptive bandwidth) and probability distribution plot (black line). Each datum is represented by a black circle on the X-axis.

The oldest population (>2 Ga) of zircons is plausibly sourced from the local Archean Gawler Craton. Late Paleoproterozoic to Mesoproterozoic (~1800-1000 Ma) zircons have several plausible sources including the Mount Isa Inlier, Mount Painter and Musgrave Provinces. The younger ca. 1200-1100 Ma peak is most likely sourced from the Musgrave Province (Wade et al. 2006, Smithies et al. 2011, Kirkland et al. 2013), as is the near 1400 Ma peak. The ca. 1600-1500 Ma peak may be sourced from any or all of the, Musgrave Province, Mount Painter Province, and/or the Mount Isa Inlier, further characterisation via geochemistry is needed to distinguish between the sources. The ca. 1700 Ma and older zircons are more likely sourced from the Mount Isa Inlier, Arunta Province or Gawler Craton. The Tonian to Cryogenian (1000-635 Ma) zircons are somewhat perplexing as there is no well documented source for these zircons in Australia. As mentioned by Reid et al. (2009) there are isolated samples from around

Australia that may account for the ca. 975-950 peak; however, it still leaves a significant age period unaccounted for. It is possible that these zircons are from Antarctica as these ages have been reported in multiple studies (Veevers and Saeed 2008, Veevers and Saeed 2011, Veevers and Saeed 2013).

The large peak in the Ediacaran to Silurian is most likely from the Delamerian and/or Lachlan Orogens (Gray and Foster 2004, Reid et al. 2009). The Carboniferous-Triassic population is most likely sourced from the northern New England Orogen (Bryan et al. 2004). The Cretaceous population is the most significant. It shows the same distinct peak as the Winton Formation, thus suggesting it is originally from the Whitsunday Volcanic Province as has been suggested by numerous studies (Veevers 2000, Bryan et al. 2012, Tucker 2014). The dominant peak is ~110 Ma, this coincides with the main pulse of volcanic activity reported by Bryan et al. (1997) for the Whitsunday Volcanic Province.

### **Hafnium Isoptic Constraints on the Provenance of the Ceduna Sub-Basin**

In addition to U-Pb data, hafnium isoptic data was collected on Gnarlyknots-1A samples. This was collected to help aid in the determination of provenance, which can, if only using U-Pb data, be problematic as multiple (but not necessarily related) terranes can show the same zircon age spectra. The use of hafnium isotope data allows for a complimentary dataset to be used to refine or delineate source regions. It may make it possible to differentiate between terranes with similar age zircons, but have different hafnium signatures. Corrected epsilon hafnium data was presented in Figure 11 and described in detail. In addition to this, several trends occur in the dataset. One noticeable and common trend throughout rocks from eastern Australia, is that the

population 800-450 Ma has continuous  $\epsilon_{\text{Hf}}$  values ranging from +4.6 to -39.9 indicating increasing source evolution over decreasing age.

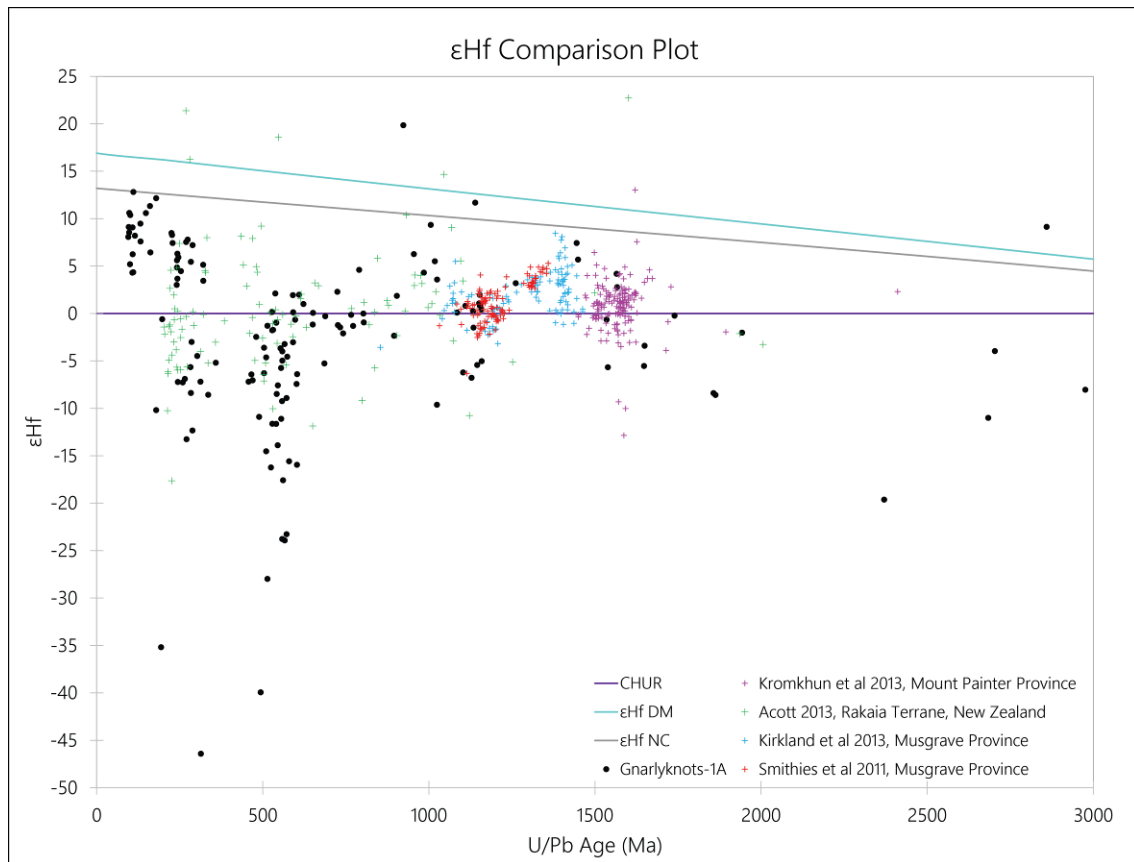


**Figure 16:** Corrected  $\epsilon_{\text{Hf}}$  values for Gnarlyknots-1A, the Rakaia Terrane in New Zealand (Acott 2013), the Musgrave Province (Smithies et al. 2011, Kirkland et al. 2013) and the Mount Painter Province (Kromkhun et al. 2013).

Figure 16 shows the corrected  $\epsilon_{\text{Hf}}$  values for several the Rakaia Terrane of New Zealand, Musgrave Province and Mount Painter Province. The similarity of the older Rakaia Terrane to the Gnarlyknots data suggests a central source for both terranes. Acott (2013) suggested several eastern Australian terranes as potential source regions for the detrital zircons in his study. The near 1500 Ma Gnarlyknots population shows a very similar to the Mount Painter Province; however, zircons of this age have been reported by previous studies (Wade et al. 2006) and should be further investigated, The ca. 1100 Ma population shows high similarity to that of the Musgrave Province. Notably both the Musgrave and Mount Painter Provinces show similar hafnium

signatures and form a near continuous dataset from ca. 1600 to ca. 1100. Although the data is not shown on Figure 16, the Mount Isa Inlier (Griffin et al. 2006), the New England Orogen (Tucker 2014) and Cretaceous zircons of the Winton Formation (Tucker 2014) all coincide with hafnium signatures at ca. 1800 Ma, ca. 300-200 Ma and ca. 150-100 Ma respectively. These additional data provide further supporting evidence that the detrital zircons found in the Upper Ceduna Delta lobe are sourced from the Australian Eastern Highlands as proposed by (Veevers 2000, King and Mee 2004).

From both U-Pb age data and hafnium isotopic data it can be argued that the sediments of the Upper Ceduna Delta lobe are sourced from a multitude of terranes, and in particular many terranes from the Eastern Australian Highlands, whilst incorporating detritus from more proximal sources along its catchment path. It is thus probable that at least the Upper (and possibly Lower) Ceduna Delta lobe is the result of a continent scale “Ceduna River”.

## **CONCLUSIONS**

This study has investigated the source of the Upper Ceduna Delta sedimentary rocks using U-Pb age and hafnium isotopic data. It has been shown that the upper lobe is sourced from the Australian Eastern Highlands, and in particular having origins in the Whitsunday Volcanic Province, most likely by a continent scale river system as originally proposed. The limitations using age only provenance was shown and the use of hafnium as a complimentary dataset has been shown to provide integral information in more accurately determining a source terrane.

## **ACKNOWLEDGMENTS**

I would like to thank my supervisors, Professor Alan Collins and Dr Stijn Glorie for their support and guidance throughout the year, particularly in the final weeks of the project. I thank the Geological Survey of South Australia for financial sponsorship of the project; I hope that this work will prove useful in future.

I would also like to thank Dr Justin Payne for his help with hafnium isotope analysis Dr Simon Holford for his assistance throughout the year and Aoife McFadden from Adelaide Microscopy for training me in use of the LA-ICP-MS for U-Pb age analysis. Finally, I would like to thank both Dr Katie Howard and Dr Rosalind King for their support throughout the year.

## REFERENCES

- "SHELL" 1975 Potoroo-1 Well Completion Report. pp. 147. Shell Development (Australia) Pty Ltd.
- ACOTT J. C. R. 2013 New Zealand where did it come from? Provenance of the Rakaia Terrane. Honours Thesis, University of Adelaide.
- ALLEY N. F., SHEARD M. J., WHITE M. R. & KRIEG G. W. 2011 The Sedimentology and Stratigraphic Significance of Cretaceous Sediments at Mt Howie, NE South Australia, *Transactions of the Royal Society of South Australia*, **135**, p. 12-25.
- BRYAN S. E., CONSTANTINE A. E., STEPHENS C. J., EWART A., SCHÖN R. W. & PARIANOS J. 1997 Early Cretaceous volcano-sedimentary successions along the eastern Australian continental margin: Implications for the break-up of eastern Gondwana, *Earth and Planetary Science Letters*, **153**, p. 85-102.
- BRYAN S. E., EWART A., STEPHENS C. J., PARIANOS J. & DOWNES P. J. 2000 The Whitsunday Volcanic Province, Central Queensland, Australia: lithological and stratigraphic investigations of a silicic-dominated large igneous province, *Journal of Volcanology and Geothermal Research*, **99**, p. 57-88.
- BRYAN S. E., ALLEN C. M., HOLCOMBE R. J. & FIELDING C. R. 2004 U–Pb zircon geochronology of Late Devonian to Early Carboniferous extension-related silicic volcanism in the northern New England Fold Belt, *Australian Journal of Earth Sciences*, **51**, p. 645-664.
- BRYAN S. E., COOK A., ALLEN C. M., SIEGEL C., PURDY D., GREENTREE J. & UYSAL T. 2012 Early-mid Cretaceous tectonic evolution of eastern Gondwana : from silicic LIP magmatism to continental rapture, *Episodes*, p. 142-152.
- COTTON T. B., SCARDINGO M. F. & BOULT P. J. 2006a. Lithostratigraphy and environments of deposition. In Alexander E. M., Sansome A. & Cotton T. B. eds. *The petroleum geology of South Australia, Vol. 2: Eromanga Basin*. 2nd ed. *Petroleum Geology of South Australia Series*, ch. 5. South Australia: Department of Primary Industries and Resources
- COTTON T. B., SCARDINGO M. F. & BOULT P. J. 2006b. Sequence stratigraphy. In Cotton T. B., Scardingo M. F. & Boulton P. J. eds. *The petroleum geology of South Australia, Vol. 2: Eromanga Basin*. 2nd ed. *Petroleum Geology of South Australia Series*, ch. 7. South Australia: Department of Primary Industries and Resources
- DHUIE B., HAWKESWORTH C. & CAWOOD P. 2011 When Continents Formed, *Science*, **331**, p. 154-155.
- GRAY D. R. & FOSTER D. A. 2004 Tectonic evolution of the Lachlan Orogen, southeast Australia: Historical review, data synthesis and modern perspectives, *Australian Journal of Earth Sciences*, **51**, p. 773-817.
- GRIFFIN W. L., BELOUSOVA E. A., WALTERS S. G. & O'REILLY S. Y. 2006 Archaean and Proterozoic crustal evolution in the Eastern Succession of the Mt Isa district, Australia: U – Pb and Hf-isotope studies of detrital zircons \*, *Australian Journal of Earth Sciences*, **53**, p. 125-149.
- HILL A. J. 1991. Revisions to the Cretaceous stratigraphic nomenclature of the Bight and Duntroon Basins, South Australia, Geological Survey of South Australia, Quarterly Geological Notes, 120, p. 2-20
- HOWARD K. E., HAND M., BAROVICH K. M., REID A., WADE B. P. & BELOUSOVA E. A. 2009 Detrital zircon ages: Improving interpretation via Nd and Hf isotopic data, *Chemical Geology*, **262**, p. 277-292.
- JACKSON S. E., PEARSON N. J., GRIFFIN W. L. & BELOUSOVA E. A. 2004 The application of laser ablation-inductively coupled plasma-mass spectrometry to in situ U–Pb zircon geochronology, *Chemical Geology*, **211**, p. 47-69.
- KING S. J. & MEE B. C. 2004 The seismic stratigraphy and petroleum potential of the Late Cretaceous Ceduna Delta, Ceduna Sub-basin, Great Australian Bight. In Boulton P. J., Johns D. R. & Lang S. C. eds. Eastern Australasian Basins Symposium II. pp. 63-73. Petroleum Exploration Society of Australia.
- KIRKLAND C. L., SMITHIES R. H., WOODHOUSE A. J., HOWARD H. M., WINGATE M. T. D., BELOUSOVA E. A., CLIFF J. B., MURPHY R. C. & SPAGGIARI C. V. 2013 Constraints and deception in the isotopic record; the crustal evolution of the west Musgrave Province, central Australia, *Gondwana Research*, **23**, p. 759-781.
- KRASSAY A. A. & TOTTERDELL J. M. 2003 Seismic stratigraphy of a large, Cretaceous shelf-margin delta complex, offshore southern Australia, *AAPG Bulletin*, **87**, p. 935-963.

- KROMKHUN K., FODEN J., HORE S. & BAINES G. 2013 Geochronology and Hf isotopes of the bimodal mafic–felsic high heat producing igneous suite from Mt Painter Province, South Australia, *Gondwana Research*, **24**, p. 1067-1079.
- LI P. F., ROSENBAUM G. & RUBATTO D. 2012 Triassic asymmetric subduction rollback in the southern New England Orogen (eastern Australia): the end of the Hunter-Bowen Orogeny, *Australian Journal of Earth Sciences*, **59**, p. 965-981.
- MACDONALD J., HOLFORD S. & KING R. 2013a. Structure and Prospectivity of the Ceduna Delta—Deep-Water Fold-Thrust Belt Systems, Bight Basin, Australia. *New Understanding of the Petroleum Systems of Continental Margins of the World: 32nd Annual*, pp. 779-816. Society of Economic Paleontologists and Mineralogists
- MACDONALD J. D. 2013 Origin and structure of the Ceduna delta system, offshore South Australia. PhD Thesis, University of Adelaide.
- MACDONALD J. D., HOLFORD S. P., GREEN P. F., DUDDY I. R., KING R. C. & BACKÉ G. 2013b Detrital zircon data reveal the origin of Australia’s largest delta system, *Journal of the Geological Society*, **170**, p. 3-6.
- PAYNE J. L., PEARSON N. J., GRANT K. J. & HALVERSON G. P. 2013 Reassessment of relative oxide formation rates and molecular interferences on in situ lutetium-hafnium analysis with laser ablation MC-ICP-MS, *Journal of Analytical Atomic Spectrometry*, **28**, p. 1068-1079.
- REID A. J., KORSCH R. J., HOU B. & BLACK L. P. 2009 Sources of sediment in the Eocene Garford paleovalley, South Australia, from detrital-zircon geochronology, *Australian Journal of Earth Sciences*, **56**, p. 125-137.
- SLÁMA J., KOŠLER J., CONDON D. J., CROWLEY J. L., GERDES A., HANCHAR J. M., HORSTWOOD M. S. A., MORRIS G. A., NASDALA L., NORBERG N., SCHALTEGGER U., SCHOENE B., TUBRETT M. N. & WHITEHOUSE M. J. 2008 Plešovice zircon — A new natural reference material for U–Pb and Hf isotopic microanalysis, *Chemical Geology*, **249**, p. 1-35.
- SMITHIES R. H., HOWARD H. M., EVINS P. M., KIRKLAND C. L., KELSEY D. E., HAND M., WINGATE M. T. D., COLLINS A. S. & BELOUSOVA E. 2011 High-Temperature Granite Magmatism, Crust-Mantle Interaction and the Mesoproterozoic Intracontinental Evolution of the Musgrave Province, Central Australia, *Journal of Petrology*, **52**, p. 931-958.
- TOTTERDELL J. M., BRADSHAW B. E. & WILLCOX J. B. 2003. The petroleum geology of South Australia. Vol. 5: Great Australian Bight. In O'Brien G. W. O. & Hibbert J. E. eds. *Great Australian Bight*, pp. 1-57. Unpublished ed. *The petroleum geology of South Australia*, ch. 4: Structural and Tectonic Setting. South Australia: Primary Industries and Resources South Australia
- TUCKER R. T., ROBERTS E. M., HU Y., KEMP A. I. S. & SALISBURY S. W. 2013 Detrital zircon age constraints for the Winton Formation, Queensland: Contextualizing Australia's Late Cretaceous dinosaur faunas, *Gondwana Research*, **24**, p. 767-779.
- TUCKER R. T. 2014 Stratigraphy, sedimentation and age of the Upper Cretaceous Winton Formation, central-western Queensland, Australia: implications for regional palaeogeography, palaeoenvironments and Gondwanan palaeontology. PhD Thesis, James Cook University.
- VEEVERS J. J. 2000. Billion-year earth history of Australia and neighbours in Gondwanaland. pp. 388. 2nd ed North Ryde, N.S.W.: GEMOC Press
- VEEVERS J. J. & SAEED A. 2008 Gamburtsev Subglacial Mountains provenance of Permian-Triassic sandstones in the Prince Charles Mountains and offshore Prydz Bay: Integrated U-Pb and TDM ages and host-rock affinity from detrital zircons, *Gondwana Research*, **14**, p. 316-342.
- VEEVERS J. J. & SAEED A. 2011 Age and composition of Antarctic bedrock reflected by detrital zircons, erratics, and recycled microfossils in the Prydz Bay-Wilkes Land-Ross Sea-Marie Byrd Land sector (70°-240°E), *Gondwana Research*, **20**, p. 710-738.
- VEEVERS J. J. & SAEED A. 2013 Age and composition of Antarctic sub-glacial bedrock reflected by detrital zircons, erratics, and recycled microfossils in the Ellsworth Land–Antarctic Peninsula–Weddell Sea–Dronning Maud Land sector (240°E–0°–015°E), *Gondwana Research*, **23**, p. 296-332.
- VERMEESCH P. 2012 On the visualisation of detrital age distributions, *Chemical Geology*, **312–313**, p. 190-194.
- WADE B. P., BAROVICH K. M., HAND M., SCRIMGEOUR I. R. & CLOSE D. F. 2006 Evidence for Early Mesoproterozoic Arc Magmatism in the Musgrave Block, Central Australia: Implications for Proterozoic Crustal Growth and Tectonic Reconstructions of Australia, *The Journal of Geology*, **114**, p. 43-63.
- WILLIS S. 2003 Gnarlyknots-1 & 1A Well Completion Report Basic Data. pp. 820. Woodside Energy Ltd.



## APPENDIX A: DETAILED METHODS

### Uranium-Lead Geochronology

U-Pb zircon geochronology was undertaken via Laser Ablation Inductively Coupled Plasma Mass Spectrometry (LA-ICP-MS). U-Pb analyses were carried out on a New Wave UP-213 laser attached to an Agilent 7500cx inductively coupled plasma mass spectrometer (ICP-MS) at Adelaide Microscopy, the University of Adelaide. Ablation was conducted in a helium atmosphere after which argon gas was added immediately to the cell to aid transport of material. A circular spot with 30- $\mu\text{m}$  diameter was chosen in order to target textural domains within the grains, while maximizing signal intensity at the mass spectrometer. A laser frequency of 5 Hz and a fluence of 3-3.3  $\text{Jcm}^{-2}$  was used at the ablation site. Background measurement of 40 seconds was conducted for each analysis, after which the laser was fired for 40 seconds with the laser shutter closed, and then ablation (laser firing, shutter open) was conducted for 50 seconds. Measured isotopes were  $^{204}\text{Pb}$ ,  $^{206}\text{Pb}$ ,  $^{207}\text{Pb}$ ,  $^{238}\text{U}$ ,  $^{208}\text{Pb}$  and  $^{232}\text{Th}$  with dwell times of 10, 15, 30, 15, 10 and 10 milliseconds respectively. Mass  $^{204}\text{Pb}$  was measured as a monitor of common lead content; however, due to the unresolvable isobaric interference of  $^{204}\text{Hg}$  on  $^{204}\text{Pb}$  common lead corrections were not conducted. Age calculations and corrections were completed in the GLITTER software through the use of the primary zircon standard GJ-1, TIMS normalization data  $^{207}\text{Pb}/^{206}\text{Pb} = 608.3 \text{ Ma}$ ,  $^{206}\text{Pb}/^{238}\text{U} = 600.7 \text{ Ma}$  and  $^{207}\text{Pb}/^{235}\text{U} = 602.2 \text{ Ma}$  (Jackson et al. 2004). An overestimated uncertainty of 1% was assigned to the TIMS derived normalization age for GJ-1. Instrument drift was also corrected for in GLITTER via standard bracketing every 15-20 unknowns and application of a linear correction. Accuracy of the methodology was verified by repeat analysis of Plešovice zircon,  $^{206}\text{Pb}/^{238}\text{U} = 337.13 \pm 0.37$  (Sláma et al. 2008). The sampling procedure was as follows, three GJ-1, two Plešovice, two GJ-1, 20 or less unknown samples, two GJ-1, two Plešovice and three GJ-1. Due to the unresolvable  $^{204}\text{Hg}$  on  $^{204}\text{Pb}$  interference, isotope ratios are presented uncorrected for common lead, with Concordia plots generated using Isoplot 4.15.

### Hafnium Isotopic Analysis

Hf analyses were completed on zircons, with previous U-Pb ages, mounted within epoxy moulds via laser ablation multi-collector inductively coupled plasma mass spectrometry (LA-MC-ICP-MS). The Hf analyses were conducted on a Thermo-Scientific Neptune Multi-collector attached to a New Wave UP-193 Excimer laser located at a joint University of Adelaide and Commonwealth Scientific and Industrial Research Organisation (CSIRO) facility at the University of Adelaide's Waite Campus. This Excimer laser delivered a beam of UV light with a wavelength of 193 nm. For analyses a circular beam with a diameter of 50  $\mu\text{m}$ , a repetition rate of 5 Hz and fluence of 7-10  $\text{J cm}^{-2}$  was chosen. A smaller 35- $\mu\text{m}$  diameter was used on a few small zircons where 50  $\mu\text{m}$  was not possible. For the analyses the  $^{171}\text{Yb}$ ,  $^{173}\text{Yb}$ ,  $^{175}\text{Lu}$ ,  $^{176}\text{Hf}$ ,  $^{177}\text{Hf}$ ,  $^{179}\text{Hf}$  and  $^{180}\text{Hf}$  were all measured concurrently. Mudtank and Plešovice zircons were used as standard to ensure accuracy. Data processing and ratio calculations were carried out using a macro-driven Excel™ workbook, HfTRaX V3.2, written by Dr. Justin Payne. Epsilon Hf,  $\text{Hf}_i$  and hafnium model ages were calculated using a modified

Excel™ workbook originally developed by the ARC National Key Centre for Geochemical Evolution and Metallogeny of Continents (GEMOC) at Macquarie University Sydney. Hafnium methods and calculations are further described in Payne et al. (2013)

## APPENDIX B: NEW U-PB AND HF ISOTOPE DATA

**Supplementary Table 1: U-Pb data collected for Gnarlyknots-1A sample 74322**

Analysis	Pb207/Pb206	$\pm 1\sigma$	Pb207/U235	$\pm 1\sigma$	Pb206/U238	$\pm 1\sigma$	Pb208/Th232 2	$\pm 1\sigma$	Rho	Concordancy	Pb207/Pb206 Age (Ma)	$\pm 1\sigma$	Pb206/U238 Age (Ma)	$\pm 1\sigma$	Pb207/U235 Age (Ma)	$\pm 1\sigma$	Pb208/Th232 Age (Ma)	$\pm 1\sigma$	Pb204 CPS	Pb206 CPS	Pb207 CPS	Pb208 CPS	Th232 CPS	U238 CPS
74322_081	0.04821	0.00267	0.10176	0.00555	0.01531	0.00028	0.00500	0.00024	0.12123	100	109.8	125.76	98	1.77	98.4	5.11	100.9	4.89	0	912	46	236	43631	77871
74322_082	0.11576	0.00143	5.12815	0.07453	0.32142	0.00433	0.09080	0.00322	0.61317	102	1891.8	22.04	1796.6	21.11	1840.8	12.35	1756.8	59.61	2	102068	12406	16626	169634	416319
74322_083	0.04974	0.00162	0.11160	0.00363	0.01628	0.00025	0.00541	0.00022	0.23329	103	183.1	73.97	104.1	1.61	107.4	3.31	109	4.46	8	2157	112	561	96467	174286
74322_084	0.05637	0.00107	0.73263	0.01472	0.09431	0.00134	0.02830	0.00113	0.42957	96	466.2	41.83	581	7.91	558.1	8.63	564	22.24	0	6253	369	858	28273	87462
74322_085	0.06933	0.00095	1.47415	0.02326	0.15428	0.00211	0.04559	0.00175	0.57519	99	908.7	28.07	924.9	11.8	919.8	9.54	901	33.77	0	24529	1779	3713	76110	210369
74322_086	0.05125	0.00104	0.34838	0.00743	0.04933	0.00071	0.01641	0.00066	0.40757	98	252.1	46.01	310.4	4.36	303.5	5.6	329	13.15	0	5648	302	1457	83241	151997
74322_087	0.05292	0.00236	0.13092	0.00576	0.01795	0.00031	0.00625	0.00031	0.16133	109	325.3	98	114.7	1.99	124.9	5.17	126	6.32	1	1133	62	268	40340	84038
74322_088	0.06029	0.00137	0.75234	0.01768	0.09055	0.00136	0.02776	0.00115	0.37041	102	614.1	48.39	558.8	8.01	569.6	10.24	553.5	22.66	0	3638	228	2713	92097	53657
74322_089	0.15512	0.00225	6.06968	0.09964	0.28395	0.00405	0.08916	0.00382	0.56062	123	2403.1	24.44	1611.2	20.31	1985.9	14.31	1726.2	70.89	8	9212	1488	2129	22572	43462
74322_090	0.06261	0.00167	0.63145	0.01704	0.07318	0.00116	0.02183	0.00104	0.31330	109	695.1	56	455.3	6.99	497	10.61	436.5	20.65	27	6073	395	1313	57021	111527
74322_091	0.08375	0.00122	2.32230	0.03885	0.20121	0.00284	0.05088	0.00226	0.56513	103	1286.6	28.26	1181.8	15.22	1219.1	11.87	1003.2	43.41	0	22200	1932	10602	198059	148745
74322_092	0.05639	0.00158	0.34467	0.00977	0.04436	0.00071	0.01526	0.00082	0.30262	107	466.8	61.39	279.8	4.36	300.7	7.38	306.2	16.39	7	4490	262	516	32289	136923
74322_093	0.06023	0.00091	0.79887	0.01378	0.09624	0.00136	0.03045	0.00147	0.55170	101	611.8	32.31	592.4	8.01	596.2	7.78	606.2	28.89	0	35505	2217	2130	66896	500489
74322_094	0.05004	0.00139	0.24642	0.00699	0.03573	0.00056	0.01074	0.00054	0.31342	99	197	63.35	226.3	3.47	223.7	5.69	216	10.86	5	3526	182	1043	93146	134312
74322_095	0.12315	0.00177	5.66719	0.09500	0.33389	0.00476	0.09418	0.00557	0.58095	104	2002.3	25.32	1857.2	23.02	1926.4	14.47	1819.2	102.81	0	77855	9919	704	7189	318355
74322_096	0.05486	0.00127	0.26540	0.00642	0.03510	0.00054	0.01165	0.00040	0.38415	107	406.3	50.78	222.4	3.36	239	5.15	234.1	8.05	0	4081	235	788	63703	162029
74322_097	0.08193	0.00119	2.11357	0.03552	0.18714	0.00273	0.06080	0.00198	0.57978	104	1243.9	28.16	1105.9	14.84	1153.2	11.58	1192.9	37.72	31	68289	5883	8498	131700	509416
74322_098	0.06178	0.00097	0.82967	0.01479	0.09742	0.00142	0.02872	0.00091	0.54596	102	666.7	33.26	599.3	8.36	613.4	8.21	572.3	17.85	0	8743	567	2475	81308	125528
74322_099	0.05896	0.00950	0.75052	0.11666	0.09234	0.00446	0.03443	0.00405	0.03546	100	565.8	316.82	569.4	26.32	568.5	67.67	684.2	79.17	0	518	32	148	4083	7860
74322_100	0.05121	0.00123	0.26416	0.00662	0.03742	0.00058	0.01178	0.00041	0.37506	101	250.5	54.46	236.8	3.6	238	5.32	236.6	8.29	1	3042	163	761	61167	114150
74322_101	0.05035	0.00166	0.26257	0.00868	0.03784	0.00064	0.01173	0.00046	0.26105	99	211	74.57	239.4	3.96	236.7	6.98	235.6	9.21	0	2486	131	618	49990	92419
74322_102	0.05073	0.00175	0.13295	0.00459	0.01901	0.00032	0.00604	0.00025	0.24545	104	228.6	77.62	121.4	2.03	126.7	4.11	121.7	5.08	0	1657	88	333	52331	122827

74322_103	0.06380	0.00095	1.03168	0.01784	0.11732	0.00172	0.03507	0.00123	0.57637	101	734.9	31.18	715.1	9.93	719.8	8.92	696.6	23.96	25	12725	850	1932	52323	153133
74322_104	0.13210	0.00161	7.05382	0.10813	0.38740	0.00560	0.11207	0.00388	0.66655	100	2126.1	21.22	2110.8	26.01	2118.2	13.63	2147	70.54	0	62067	8583	9153	77662	226628
74322_105	0.20450	0.00249	15.68730	0.24034	0.55654	0.00806	0.15587	0.00551	0.66749	100	2862.4	19.63	2852.3	33.4	2857.9	14.62	2927.7	96.37	15	59327	12692	9044	55246	151077
74322_106	0.11069	0.00152	3.82243	0.06290	0.25054	0.00370	0.07836	0.00290	0.61788	111	1810.8	24.75	1441.3	19.06	1597.5	13.24	1524.9	54.27	3	22513	2605	3693	44929	127593
74322_107	0.06823	0.00107	1.27169	0.02297	0.13523	0.00202	0.04086	0.00155	0.56235	102	875.4	32.24	817.6	11.45	833.1	10.27	809.5	30.1	0	11859	845	2317	54135	124764
74322_108	0.08945	0.00122	2.97702	0.04904	0.24145	0.00355	0.06944	0.00263	0.62244	101	1413.8	25.79	1394.2	18.46	1401.8	12.52	1357	49.64	2	35594	3324	11102	152807	210128
74322_109	0.10112	0.00127	3.86792	0.06099	0.27750	0.00405	0.05690	0.00218	0.66028	102	1644.9	23.15	1578.7	20.41	1607	12.72	1118.5	41.76	12	109790	11585	36910	620838	565016
74322_110	0.07835	0.00119	2.10357	0.03730	0.19478	0.00292	0.05808	0.00230	0.58022	100	1155.8	29.89	1147.2	15.74	1150	12.2	1141	43.9	0	12472	1019	7115	117417	91623
74322_111	0.07223	0.00499	1.75283	0.11664	0.17605	0.00486	0.05644	0.00413	0.11362	98	992.5	134.36	1045.3	26.64	1028.2	43.02	1109.7	79.03	5	810	61	189	3228	6601
74322_112	0.05113	0.00088	0.30024	0.00583	0.04261	0.00064	0.01328	0.00056	0.52533	99	246.5	39.08	269	3.97	266.6	4.55	266.7	11.24	6	9413	501	1615	116836	317350
74322_113	0.04991	0.00384	0.10764	0.00810	0.01565	0.00038	0.00565	0.00035	0.09105	104	190.8	169.85	100.1	2.42	103.8	7.42	113.8	6.93	0	703	36	218	37204	64742
74322_114	0.16678	0.00232	10.86797	0.18335	0.47272	0.00710	0.13002	0.00567	0.62493	101	2525.6	23.17	2495.5	31.1	2511.9	15.69	2470.6	101.47	0	18919	3282	4210	31194	57707
74322_115	0.05711	0.00132	0.64343	0.01571	0.08173	0.00130	0.02403	0.00110	0.40545	100	495.2	50.62	506.4	7.78	504.4	9.7	480.1	21.79	0	3663	217	1186	47626	64757
74322_116	0.06913	0.00129	1.40119	0.02889	0.14703	0.00229	0.04417	0.00213	0.49743	101	902.6	37.93	884.3	12.88	889.4	12.22	873.6	41.3	3	16969	1218	1908	41728	167057
74322_117	0.06036	0.00090	0.82860	0.01476	0.09958	0.00151	0.03002	0.00107	0.60146	100	616.4	31.98	611.9	8.84	612.8	8.2	597.7	20.96	0	12736	795	796	26617	187151
74322_118	0.05077	0.00108	0.27737	0.00640	0.03962	0.00062	0.01195	0.00041	0.44972	99	230.6	48.6	250.5	3.87	248.6	5.08	240	8.09	8	4405	231	1864	157109	162821
74322_119	0.05079	0.00165	0.22158	0.00732	0.03164	0.00054	0.00981	0.00037	0.29020	101	231.3	73.32	200.8	3.37	203.2	6.08	197.3	7.5	18	1637	86	496	51160	75855
74322_120	0.04788	0.00371	0.11439	0.00874	0.01733	0.00038	0.00557	0.00032	0.09389	99	92.2	174.86	110.8	2.43	110	7.96	112.3	6.41	0	516	25	118	21662	43707
74322_121	0.04981	0.00295	0.13066	0.00757	0.01903	0.00042	0.00595	0.00033	0.13144	103	186	132.49	121.5	2.67	124.7	6.8	120	6.72	0	1217	62	273	46791	93952
74322_122	0.04803	0.00112	0.11045	0.00274	0.01668	0.00027	0.00516	0.00020	0.41547	100	100.7	54.14	106.6	1.69	106.4	2.5	104	3.96	0	3361	166	767	151972	296026
74322_123	0.18982	0.00257	13.81808	0.23142	0.52801	0.00813	0.15068	0.00566	0.64811	100	2740.6	22.11	2733	34.32	2737.3	15.86	2836.9	99.4	12	25581	5022	3992	27160	71235
74322_124	0.05782	0.00088	0.69408	0.01257	0.08707	0.00133	0.02671	0.00103	0.59586	99	522.7	33.3	538.2	7.87	535.2	7.54	532.8	20.2	0	16109	963	1762	67873	272234
74322_125	0.05876	0.00095	0.78229	0.01472	0.09657	0.00148	0.03067	0.00119	0.56792	99	558.2	35.13	594.3	8.72	586.8	8.39	610.6	23.26	14	12371	751	2727	91805	188675
74322_126	0.05297	0.00195	0.25680	0.00947	0.03516	0.00064	0.01155	0.00052	0.25029	104	327.5	81.4	222.8	3.96	232.1	7.65	232.1	10.41	0	1596	87	464	41723	66911
74322_127	0.06018	0.00092	0.81114	0.01478	0.09776	0.00150	0.03030	0.00124	0.59685	100	610.1	32.82	601.3	8.78	603.1	8.29	603.4	24.24	0	15234	947	2033	69792	229856
74322_128	0.08011	0.00136	2.30474	0.04476	0.20868	0.00327	0.06407	0.00265	0.54959	99	1199.7	33.09	1221.8	17.47	1213.7	13.75	1255.2	50.4	0	11070	916	4282	69774	78314
74322_129	0.07674	0.00174	2.06379	0.04959	0.19505	0.00327	0.05903	0.00262	0.42738	99	1114.6	44.59	1148.7	17.62	1136.9	16.43	1159.3	50.06	0	11124	882	3404	60429	84264

74322_130	0.06939	0.00119	1.38346	0.02722	0.14461	0.00226	0.04581	0.00202	0.54840	101	910.4	35.05	870.7	12.74	881.9	11.59	905.3	39.02	1	9750	699	1994	45796	99700
74322_131	0.05543	0.00245	0.40324	0.01760	0.05276	0.00105	0.01618	0.00096	0.20000	104	429.4	95.66	331.5	6.42	344	12.74	324.5	19.06	0	1365	78	238	15577	38296
74322_132	0.05146	0.00145	0.22768	0.00664	0.03209	0.00054	0.01080	0.00051	0.34614	102	261.5	63.57	203.6	3.38	208.3	5.49	217.1	10.24	0	2950	156	1060	104041	136171
74322_133	0.12475	0.00172	6.32188	0.10829	0.36756	0.00561	0.10940	0.00507	0.64311	100	2025.3	24.22	2017.9	26.46	2021.5	15.02	2098.4	92.37	7	32342	4168	6617	64335	130433
74322_134	0.18146	0.00408	12.12227	0.28490	0.48456	0.00905	0.13480	0.00787	0.45066	103	2666.2	36.8	2547.1	39.3	2613.9	22.05	2555.9	140.23	20	32353	6065	4176	33079	99055
74322_135	0.05810	0.00168	0.76373	0.02262	0.09535	0.00166	0.03053	0.00161	0.33376	98	532.9	62.03	587.1	9.75	576.2	13.02	607.9	31.56	0	5009	300	1244	43668	78007

Supplementary Table 2: U-Pb data collected for Hughes-2 sample 106988																								
Analysis	Pb207/Pb206	± 1σ	Pb207/U235	± 1σ	Pb206/U238	± 1σ	Pb208/Th232	± 1σ	Rho	Concordancy	Pb207/Pb206 Age (Ma)	± 1σ	Pb206/U238 Age (Ma)	± 1σ	Pb207/U235 Age (Ma)	± 1σ	Pb208/Th232 Age (Ma)	± 1σ	Pb204 CPS	Pb206 CPS	Pb207 CPS	Pb208 CPS	Th232 CPS	U238 CPS
106988_02	0.0706	0.00349	2.09646	0.10312	0.21613	0.00538	0.05519	0.01207	0.243138056	91	945.9	98.09	1261.4	28.54	1147.6	33.81	1085.8	231.22	0	2544	210	1119	19965	18453
106988_03	0.07145	0.00416	1.85602	0.09606	0.18927	0.00431	0.07203	0.0232	0.081725721	95	970.4	114.43	1117.4	23.36	1065.6	34.15	1405.9	437.46	0	7495	575	6181	103588	50104
106988_04	0.09821	0.0031	3.55807	0.10823	0.26223	0.00458	0.08472	0.01497	0.220190704	103	1590.4	57.76	1501.3	23.41	1540.2	24.11	1643.7	278.9	9	14437	1559	3954	53508	76269
106988_05	0.07632	0.00289	1.88027	0.06569	0.17836	0.00324	0.0737	0.01481	0.091896709	102	1103.5	73.88	1058	17.7	1074.2	23.16	1437.2	278.74	0	3278	270	1499	25119	24026
106988_06	0.09758	0.00552	3.06008	0.15494	0.22785	0.00518	0.04144	0.00891	0.051922403	108	1578.4	102.22	1323.2	27.18	1422.8	38.75	820.7	172.9	10	24513	2576	3871	75369	139837
106988_07	0.07439	0.00204	2.02463	0.05433	0.19702	0.00323	0.07054	0.01048	0.269178929	97	1052	54.39	1159.3	17.39	1123.8	18.24	1377.7	197.79	11	25094	2027	8019	129316	175096
106988_08	0.09759	0.00283	3.91739	0.11276	0.29078	0.00508	0.07561	0.00897	0.291148536	98	1578.6	53.29	1645.4	25.36	1617.3	23.28	1473.3	168.53	8	13314	1418	3059	35619	65690
106988_09	0.07671	0.00204	2.1719	0.05735	0.20513	0.00339	0.06274	0.00752	0.301500384	97	1113.6	52.1	1202.8	18.13	1172.1	18.36	1230	143.07	10	5779	478	3100	52891	39299
106988_10	0.07639	0.00364	2.03961	0.09055	0.19426	0.00416	0.05397	0.00901	0.083633667	99	1105.2	92.37	1144.4	22.46	1128.8	30.25	1062.4	172.71	2	4201	349	2874	46789	28788
106988_11	0.09686	0.00206	3.89881	0.08594	0.29169	0.00455	0.09328	0.00917	0.402630118	98	1564.5	39.41	1649.9	22.73	1613.4	17.81	1802.5	169.62	6	20455	2139	3703	41167	98451
106988_12	0.07227	0.00146	1.76134	0.0378	0.1767	0.00277	0.05691	0.00487	0.443179872	98	993.5	40.57	1048.9	15.18	1031.3	13.9	1118.7	93.15	0	15888	1242	6518	114626	128627
106988_13	0.09115	0.00345	3.94498	0.15801	0.31627	0.00717	0.06896	0.01062	0.37753629	92	1449.7	70.45	1771.5	35.14	1623	32.44	1347.8	200.9	0	34639	3591	6759	84795	185927
106988_14	0.0795	0.00153	2.18311	0.04497	0.19909	0.00308	0.05204	0.00365	0.460143878	100	1184.6	37.54	1170.4	16.56	1175.7	14.34	1025.5	70.08	0	8300	706	2152	40760	59206
106988_15	0.08703	0.00274	2.4859	0.08016	0.20779	0.00422	0.05237	0.0046	0.352007703	104	1361.2	59.4	1217	22.53	1267.9	23.35	1031.7	88.27	38	4090	399	2712	45483	31728
106988_16	0.07442	0.00132	2.15967	0.04212	0.21046	0.00322	0.05889	0.00323	0.502432226	95	1052.8	35.32	1231.3	17.17	1168.2	13.54	1156.6	61.68	1	7780	616	3631	59987	52804
106988_17	0.09353	0.00297	2.6578	0.08501	0.20631	0.00415	0.04842	0.00326	0.325870638	109	1498.5	58.95	1209.1	22.19	1316.8	23.6	955.7	62.87	0	3026	307	1934	34195	22963
106988_18	0.07578	0.00116	2.07791	0.03643	0.19883	0.00295	0.05864	0.00261	0.563557406	98	1089.4	30.36	1169	15.88	1141.5	12.02	1151.8	49.89	16	12049	966	6191	105381	85928

Jarred Cain Lloyd  
Provenance of the Upper Ceduna Delta Lobe

106988_19	0.07654	0.00135	2.11664	0.04108	0.20054	0.00306	0.05764	0.00231	0.503829519	98	1109.3	34.82	1178.2	16.46	1154.2	13.38	1132.7	44.05	1	5245	423	3340	57428	37156
106988_20	0.07587	0.00128	2.03872	0.03833	0.19493	0.00293	0.05592	0.00211	0.521553559	98	1091.6	33.46	1148	15.82	1128.5	12.81	1099.7	40.44	1	6823	541	3647	63372	49383
106988_21	0.10252	0.00244	3.71529	0.09332	0.26327	0.00469	0.05882	0.00403	0.426639057	105	1670.2	43.45	1506.6	23.93	1574.7	20.09	1155.2	76.95	36	28596	3079	8214	127242	167608
106988_22	0.07898	0.00099	2.1602	0.03434	0.19839	0.00295	0.03896	0.00104	0.669879464	100	1171.6	24.54	1166.7	15.88	1168.3	11.03	772.4	20.17	8	20392	1675	8752	213632	149725
106988_23	0.10306	0.00142	2.73651	0.04679	0.19257	0.00295	0.04489	0.00173	0.643652793	118	1679.9	25.32	1135.3	15.94	1338.4	12.72	887.6	33.41	42	57625	6142	18522	386439	444116
106988_24	0.10173	0.00131	4.0436	0.06479	0.2883	0.00429	0.07764	0.00217	0.654991497	101	1656	23.6	1633	21.49	1643	13.04	1511.3	40.76	8	14290	1512	5604	68561	71677
106988_25	0.1009	0.00128	3.72132	0.06006	0.26756	0.00404	0.0696	0.00213	0.672032877	103	1640.7	23.33	1528.4	20.53	1576	12.92	1359.9	40.24	23	26387	2765	4143	56001	145161
106988_26	0.07843	0.00113	2.02782	0.03487	0.18754	0.00282	0.05754	0.00169	0.607606909	102	1157.8	28.39	1108.1	15.29	1124.9	11.69	1130.7	32.23	25	10007	816	5763	94820	77036
106988_27	0.16385	0.00357	2.54175	0.05855	0.11251	0.00195	0.04063	0.00242	0.446206683	187	2495.8	36.27	687.3	11.31	1284.1	16.78	804.9	46.96	114	16128	2696	22247	495983	215613
106988_28	0.07798	0.00114	2.1586	0.03738	0.2008	0.00301	0.05644	0.00176	0.59876345	99	1146.4	28.79	1179.6	16.18	1167.8	12.02	1109.8	33.64	1	10208	828	4127	69444	73219
106988_29	0.07574	0.00101	2.01511	0.03324	0.19299	0.00288	0.0565	0.00179	0.64382611	99	1088.3	26.53	1137.6	15.58	1120.6	11.19	1110.9	34.24	12	21152	1667	9891	164731	159350
106988_30	0.07726	0.001	2.06558	0.03318	0.19396	0.00286	0.0514	0.00165	0.650017931	100	1127.8	25.47	1142.8	15.45	1137.5	10.99	1013.1	31.66	7	24405	1961	8094	149302	181322
106988_31	0.0794	0.00123	2.01485	0.03643	0.18411	0.00282	0.05786	0.00187	0.580528741	103	1182	30.3	1089.4	15.35	1120.5	12.27	1137	35.72	0	8074	667	3495	56863	63968
106988_32	0.08652	0.00202	0.90044	0.02205	0.0755	0.00128	0.03449	0.002	0.411885269	139	1349.9	44.33	469.2	7.68	652	11.78	685.4	39.02	13	11951	1080	5586	150247	235834
106988_33	0.0847	0.00131	1.67537	0.03041	0.14351	0.0022	0.03223	0.00143	0.58446974	116	1308.7	29.84	864.5	12.39	999.2	11.54	641.2	28.08	4	28063	2478	10903	319876	285954
106988_34	0.07771	0.00145	2.20064	0.04599	0.20539	0.0033	0.05532	0.00303	0.516314465	98	1139.5	36.79	1204.2	17.65	1181.2	14.59	1088.3	58.04	0	28214	2292	15169	254597	204892
106988_35	0.0809	0.00182	2.24564	0.05263	0.20147	0.00326	0.05789	0.00268	0.402115295	101	1218.9	43.51	1183.2	17.49	1195.4	16.47	1137.4	51.27	4	4125	347	2084	34569	28912
106988_36	0.08476	0.00418	2.33937	0.11107	0.20031	0.00479	0.05792	0.00373	0.173516882	104	1310	92.93	1177	25.72	1224.3	33.77	1138.1	71.21	9	1070	95	578	9520	7617
106988_37	0.07689	0.00166	2.13602	0.04915	0.20153	0.00329	0.05562	0.00209	0.439082867	98	1118.5	42.52	1183.5	17.64	1160.5	15.91	1094	40.01	10	2714	217	1061	17929	19603
106988_38	0.07866	0.00139	2.0881	0.04143	0.19258	0.00302	0.05365	0.00201	0.525997268	101	1163.7	34.72	1135.3	16.31	1144.9	13.62	1056.3	38.49	14	4801	392	1381	24217	36383
106988_39	0.08052	0.00169	2.13804	0.04787	0.19266	0.00312	0.05394	0.00214	0.445457826	102	1209.7	40.72	1135.8	16.85	1161.2	15.49	1061.9	40.99	9	3125	262	1645	28519	23498
106988_40	0.07553	0.00141	2.04546	0.04219	0.19649	0.0031	0.05651	0.00213	0.500668418	98	1082.6	36.95	1156.4	16.72	1130.8	14.07	1111.1	40.8	5	4305	338	3207	53296	32014
106988_41	0.07839	0.00135	2.11252	0.04106	0.19548	0.00305	0.05361	0.00171	0.535243705	100	1156.8	33.84	1151	16.45	1152.9	13.4	1055.6	32.73	0	4934	402	3380	59434	36868
106988_42	0.07945	0.0014	2.17001	0.04274	0.19813	0.00309	0.05604	0.00203	0.521936151	101	1183.3	34.54	1165.3	16.65	1171.5	13.69	1102.1	38.81	7	5344	443	1508	25479	39210
106988_43	0.07566	0.00118	2.02176	0.03707	0.1938	0.003	0.05402	0.00196	0.585875109	98	1086.2	31.05	1141.9	16.19	1122.9	12.46	1063.4	37.56	10	11234	883	5035	87877	85616
106988_44	0.07659	0.0012	2.04848	0.03734	0.19399	0.00298	0.05573	0.00196	0.576334783	99	1110.5	30.91	1143	16.07	1131.8	12.44	1096.2	37.57	0	7978	635	3433	58605	60183
106988_45	0.07745	0.00129	2.09895	0.03983	0.19654	0.00305	0.05553	0.00205	0.54926844	99	1132.9	32.7	1156.7	16.42	1148.5	13.05	1092.3	39.23	11	6184	497	1963	33656	46062

106988_46	0.07647	0.0027	2.01648	0.06997	0.19152	0.00366	0.06362	0.00581	0.243230341	99	1107.3	69.07	1129.6	19.81	1121.1	23.55	1246.6	110.41	0	6111	483	1758	28594	45611
106988_47	0.09173	0.00166	2.50196	0.0513	0.19773	0.00319	0.06789	0.00412	0.533872663	109	1461.8	34.14	1163.1	17.15	1272.6	14.87	1327.7	77.89	16	34866	3306	3393	47931	266481
106988_48	0.08295	0.00157	2.34799	0.04657	0.20524	0.00298	0.06944	0.00396	0.427061823	102	1268.1	36.47	1203.4	15.94	1226.9	14.13	1357	74.86	0	17835	1552	3152	46916	113705
106988_49	0.07804	0.00132	2.11513	0.03996	0.19664	0.00296	0.05919	0.00195	0.522911257	100	1147.8	33.3	1157.3	15.94	1153.8	13.02	1162.4	37.16	0	7534	608	2955	49324	53937
106988_50	0.10758	0.00286	4.59122	0.12204	0.30976	0.00538	0.08224	0.00497	0.326489924	100	1758.8	47.8	1739.5	26.48	1747.7	22.16	1597.5	92.76	0	6421	709	2224	26691	28039
106988_51	0.07876	0.00155	2.0605	0.04331	0.18982	0.00293	0.062	0.00238	0.451172796	101	1166.1	38.43	1120.4	15.86	1135.8	14.37	1215.9	45.21	22	6150	500	3133	50824	45250
106988_52	0.09901	0.00127	3.88091	0.06021	0.28438	0.00403	0.08822	0.00283	0.629925204	100	1605.6	23.76	1613.4	20.22	1609.7	12.53	1708.9	52.65	12	17136	1748	6135	68413	82914
106988_53	0.0784	0.00104	2.02351	0.03191	0.18725	0.00264	0.06317	0.00224	0.610546285	102	1157.1	25.97	1106.5	14.35	1123.4	10.72	1238.1	42.61	0	26802	2169	8894	139147	196569
106988_54	0.07822	0.00127	2.08764	0.0377	0.19364	0.00281	0.0616	0.00219	0.52103423	100	1152.4	31.82	1141.1	15.17	1144.8	12.4	1208.3	41.65	0	6893	554	3432	54580	48665
106988_55	0.07827	0.00171	1.92538	0.04316	0.17841	0.00269	0.05605	0.00354	0.373561509	103	1153.8	42.69	1058.3	14.7	1089.9	14.98	1102.3	67.74	5	12522	1015	5141	87578	92585
106988_56	0.09827	0.00175	3.71682	0.07443	0.27447	0.00431	0.09113	0.00496	0.525454979	101	1591.6	32.93	1563.5	21.78	1575	16.02	1762.9	91.83	0	23716	2380	12188	135796	126188
106988_57	0.07641	0.00204	2.02032	0.05425	0.19184	0.00311	0.0573	0.00329	0.311342939	99	1105.7	52.48	1131.3	16.84	1122.4	18.24	1126.2	62.84	1	3833	300	1462	24317	26618
106988_58	0.08074	0.00152	2.18477	0.04572	0.19632	0.00311	0.06484	0.00394	0.504458465	102	1215.1	36.56	1155.5	16.78	1176.2	14.58	1269.9	74.84	3	31404	2601	9959	153975	236061
106988_59	0.0793	0.0016	2.03463	0.04365	0.18615	0.00283	0.05862	0.00248	0.435816122	102	1179.5	39.45	1100.5	15.4	1127.2	14.6	1151.4	47.35	7	3691	298	2084	34518	27229
106988_60	0.07927	0.00281	2.10832	0.07403	0.19297	0.00375	0.05964	0.00621	0.259388446	101	1179	68.58	1137.4	20.29	1151.5	24.18	1170.8	118.38	0	9991	821	3717	65758	75810
106988_61	0.08121	0.00193	2.09935	0.05278	0.18772	0.00316	0.05397	0.0045	0.414262195	104	1226.5	46.04	1109	17.17	1148.6	17.29	1062.4	86.33	15	28716	2396	10540	199734	228493
106988_62	0.10245	0.00152	4.0405	0.06955	0.28615	0.00415	0.08112	0.00364	0.573836489	101	1669	27.22	1622.3	20.8	1642.4	14.01	1576.5	68	0	13058	1358	2422	28943	63215
106988_63	0.081	0.0024	2.13167	0.06281	0.1908	0.00319	0.05433	0.00484	0.27384462	103	1221.5	57	1125.7	17.26	1159.1	20.37	1069.3	92.84	0	7397	606	2823	48036	51000

SUPPLEMENTARY TABLE 3: HF DATA COLLECTED FOR GNARLYKNOTS-1A, SAMPLE 74318

Sample Number	176Hf/177Hf	2 $\sigma$	Hf fract	178Hf/177Hf	2 $\sigma$	176Lu/177Hf	2 $\sigma$	176Yb/177Hf	2 $\sigma$	U/Pb Age (Ma)	2 $\sigma$ Error	Hf <sub>i</sub>	$\epsilon$ Hf	2 $\sigma$ Error
74318-02	0.282434	0.000042	0.897779	1.467357	0.000259	0.002067	0.000060	0.076897	0.000409	265.3	9.12	0.282424	-6.89	2.92
74318-06	0.282801	0.000030	0.909009	1.467392	0.000384	0.000689	0.000028	0.024532	0.001420	246	7.28	0.282798	5.93	2.12
74318-08	0.281878	0.000057	0.876210	1.467200	0.000351	0.000652	0.000040	0.028453	0.002749	1024.3	32.54	0.281866	-9.62	3.99
74318-12	0.282755	0.000175	0.889316	1.466899	0.001352	0.000712	0.000032	0.029122	0.001664	253.5	8.24	0.282752	4.47	12.25
74318-13	0.282394	0.000070	0.872351	1.467352	0.000480	0.001484	0.000083	0.055248	0.000567	312.3	11.58	0.282386	-7.19	4.93
74318-17	0.282102	0.000124	-0.899174	1.467844	0.000633	0.000902	0.000073	0.031424	0.001581	1444.6	45.66	0.282077	7.44	8.68

74318-18	0.282769	0.000086	0.867824	1.467221	0.000493	0.001470	0.000039	0.058458	0.001916	283.4	13.1	0.282761	5.45	6.03
74318-19	0.281686	0.000082	0.852077	1.467279	0.000598	0.000467	0.000007	0.015274	0.000844	1739.4	59.72	0.281671	-0.23	5.74
74318-20	0.282841	0.000047	-0.808364	1.467286	0.000442	0.000944	0.000016	0.033927	0.001781	109.7	3.76	0.282839	4.35	3.32
74318-23	0.283082	0.000084	-0.821824	1.467186	0.000599	0.001770	0.000063	0.058978	0.003389	110.4	4.06	0.283078	12.82	5.85
74318-27	0.281928	0.000114	-0.810530	1.467293	0.000710	0.000982	0.000102	0.034151	0.003914	1145.2	35.54	0.281906	-5.43	7.95
74318-28	0.282737	0.000055	-0.815497	1.467199	0.000429	0.001308	0.000045	0.037846	0.001401	320.3	10.74	0.282729	5.14	3.84
74318-32	0.282179	0.000047	-0.793840	1.467323	0.000464	0.000973	0.000043	0.030310	0.000344	488.8	19.66	0.282170	-10.89	3.30
74318-33	0.282920	0.000047	-0.826019	1.467171	0.000420	0.001077	0.000083	0.030876	0.002580	132	6.1	0.282917	7.60	3.30
74318-34	0.282316	0.000033	-0.785151	1.467258	0.000327	0.000574	0.000009	0.022079	0.000122	465.5	20.52	0.282311	-6.42	2.31
74318-37	0.282253	0.000078	0.878651	1.467461	0.000783	0.000802	0.000030	0.032836	0.001053	1024.5	41.9	0.282238	3.59	5.44
74318-39	0.282429	0.000061	-0.927807	1.467270	0.000461	0.000728	0.000036	0.028871	0.001706	622.5	25.5	0.282421	1.00	4.25
74318-40	0.282132	0.000048	-0.913327	1.467276	0.000434	0.000977	0.000034	0.038482	0.000827	555.3	22.98	0.282122	-11.10	3.35
74318-43	0.282208	0.000040	-0.850113	1.467426	0.000280	0.001015	0.000050	0.028978	0.001078	601.4	15.76	0.282196	-7.43	2.78
74318-49	0.282424	0.000039	0.924021	1.467385	0.000274	0.001495	0.000092	0.050319	0.001905	259	8.86	0.282417	-7.27	2.73
74318-51	0.282427	0.000057	0.848009	1.467623	0.000606	0.000249	0.000005	0.009807	0.000225	514	18.8	0.282425	-1.29	4.00
74318-53	0.282403	0.000035	0.861183	1.467179	0.000207	0.000743	0.000043	0.026930	0.001261	724.2	22.64	0.282393	2.30	2.44
74318-58	0.282103	0.000027	0.873631	1.467368	0.000353	0.000467	0.000006	0.015312	0.000082	1139.2	34.5	0.282393	11.68	1.88

SUPPLEMENTARY TABLE 4: HF DATA COLLECTED FOR GNARLYKNOTS-1A, SAMPLE 74319

Sample Number	<sup>176</sup> Hf/ <sup>177</sup> Hf	2σ	Hf fract	<sup>178</sup> Hf/ <sup>177</sup> Hf	2σ	<sup>176</sup> Lu/ <sup>177</sup> Hf	2σ	<sup>176</sup> Yb/ <sup>177</sup> Hf	2σ	U/Pb Age (Ma)	2σ Error	Hfi	εHf	2σ Error
74319-02	0.282301	0.000029	0.875949	1.467441	0.000386	0.000548	0.000006	0.021515	0.000408	573.7	15.24	0.282295	-4.56	2.01
74319-06	0.281959	0.000029	0.886396	1.467226	0.000230	0.000387	0.000004	0.014638	0.000289	602.9	16.04	0.281955	-15.95	2.04
74319-07	0.282461	0.000020	0.904352	1.467200	0.000129	0.000392	0.000005	0.014113	0.000164	527.3	13.6	0.282458	0.16	1.37
74319-10	0.281987	0.000025	0.883311	1.467263	0.000210	0.000644	0.000013	0.025825	0.000239	579	15.82	0.281980	-15.58	1.76
74319-11	0.282946	0.000026	0.886059	1.467178	0.000274	0.000616	0.000010	0.023041	0.000139	115	6.12	0.282945	8.21	1.80
74319-12	0.282338	0.000026	0.886882	1.467342	0.000197	0.000997	0.000015	0.034654	0.001075	335.6	9.14	0.282332	-8.58	1.85
74319-13	0.281923	0.000019	0.887033	1.467220	0.000170	0.000540	0.000010	0.018999	0.000158	1103.1	32.92	0.281911	-6.21	1.36
74319-15	0.281278	0.000017	0.909211	1.467319	0.000160	0.000244	0.000002	0.008570	0.000109	313.8	11.06	0.281276	-46.41	1.22
74319-16	0.282233	0.000059	0.761224	1.467586	0.000527	0.000520	0.000031	0.015063	0.000699	545.3	16.48	0.282228	-7.57	4.14
74319-17	0.282276	0.000016	0.890028	1.467224	0.000169	0.000200	0.000005	0.007532	0.000131	554.8	23.4	0.282273	-5.74	1.09



74319-20	0.282296	0.000020	0.899187	1.467284	0.000170	0.000355	0.000005	0.015544	0.000179	558.9	21.32	0.282292	-4.97	1.39
74319-21	0.282072	0.000024	0.899275	1.467313	0.000296	0.000406	0.000004	0.015528	0.000184	1158.1	34.88	0.282063	0.42	1.70
74319-22	0.282278	0.000038	0.853838	1.467340	0.000380	0.000662	0.000031	0.025831	0.000655	903.4	28.16	0.282267	1.86	2.67
74319-24	0.281912	0.000030	0.929756	1.467258	0.000230	0.001519	0.000019	0.049711	0.000590	1566.5	58.22	0.281867	2.78	2.13
74319-25	0.282857	0.000026	0.928854	1.467256	0.000298	0.001296	0.000046	0.050330	0.001244	228.4	7.6	0.282852	7.43	1.83
74319-26	0.282365	0.000070	0.878351	1.467584	0.000385	0.001696	0.000076	0.069251	0.001475	687.9	18.46	0.282343	-0.28	4.88
74319-35	0.282868	0.000034	-0.874274	1.467337	0.000261	0.000887	0.000044	0.030816	0.001982	161.6	5.74	0.282866	6.44	2.39
74319-37	0.282648	0.000070	-0.876816	1.467311	0.000616	0.001051	0.000050	0.043886	0.003538	197	6.78	0.282644	-0.60	4.91
74319-40	0.281234	0.000069	-0.872607	1.467649	0.000507	0.000592	0.000024	0.017960	0.001142	2859.7	73.2	0.281201	9.14	4.85
74319-41	0.282843	0.000069	-0.858615	1.467601	0.000439	0.001738	0.000079	0.052542	0.000632	107.5	5.3	0.282840	4.31	4.86
74319-42	0.282135	0.000034	-0.883686	1.467263	0.000259	0.001127	0.000023	0.037430	0.001122	1152.8	35.42	0.282110	1.97	2.35
74319-45	0.282423	0.000024	-0.927479	1.467445	0.000218	0.000452	0.000040	0.018000	0.001859	790.1	28.22	0.282416	4.61	1.70
74319-48	0.282455	0.000048	-0.915793	1.467359	0.000297	0.001310	0.000043	0.045812	0.002334	282.3	9.6	0.282448	-5.65	3.34
74319-51	0.282304	0.000023	-0.908343	1.467310	0.000197	0.001164	0.000022	0.041777	0.001303	457	15.56	0.282294	-7.18	1.64
74319-55	0.282462	0.000023	-0.913100	1.467312	0.000151	0.000415	0.000022	0.016134	0.000963	609.2	22.6	0.282457	1.98	1.58
74319-59	0.282228	0.000022	-0.914332	1.467363	0.000307	0.000293	0.000004	0.011585	0.000471	603.1	23.86	0.282224	-6.39	1.56
74319-65	0.282881	0.000032	-0.917761	1.467425	0.000219	0.001069	0.000112	0.035358	0.001569	226.8	10.62	0.282877	8.29	2.25
74319-66	0.281651	0.000026	-0.833370	1.467516	0.000510	0.000118	0.000004	0.004335	0.000057	1538.8	71.48	0.281647	-5.66	1.81
74319-68	0.282975	0.000025	0.933812	1.467277	0.000186	0.000497	0.000041	0.018057	0.001804	107.8	5.66	0.282974	9.07	1.76
74319-69	0.282100	0.000028	-0.874790	1.467440	0.000217	0.000621	0.000022	0.021440	0.001025	1151.3	49.52	0.282086	1.08	1.95
74319-77	0.282046	0.000043	-0.829241	1.467450	0.000248	0.000762	0.000094	0.020826	0.003424	1448.8	62.58	0.282025	5.69	3.01
74319-78	0.282378	0.000069	0.918142	1.467365	0.000295	0.001412	0.000072	0.051862	0.005013	283.4	13.98	0.282370	-8.37	4.85
74319-80	0.282208	0.000023	-0.915928	1.467320	0.000279	0.000326	0.000012	0.012285	0.000676	541.8	24.56	0.282204	-8.47	1.62

SUPPLEMENTARY TABLE 5: HF DATA COLLECTED FOR GNARLYKNOTS-1A, SAMPLE 74321

Sample Number	176Hf/177Hf	2 $\sigma$	Hf fract	178Hf/177Hf	2 $\sigma$	176Lu/177Hf	2 $\sigma$	176Yb/177Hf	2 $\sigma$	U/Pb Age (Ma)	2 $\sigma$ Error	Hfi	$\epsilon$ Hf	2 $\sigma$ Error
74321-03	0.282117	0.000018	0.901993	1.467251	0.000152	0.000078	0.000007	0.003569	0.000346	540.3	15.56	0.282116	-11.64	1.29
74321-08	0.282895	0.000020	0.901119	1.467364	0.000189	0.000474	0.000017	0.015389	0.000254	108.3	4.92	0.282894	6.25	1.38
74321-10	0.282776	0.000029	0.879703	1.467444	0.000208	0.001068	0.000063	0.033376	0.000686	241.4	8.44	0.282771	4.86	2.01
74321-11	0.282292	0.000015	0.889741	1.467223	0.000122	0.000920	0.000009	0.035757	0.000659	802.7	20.38	0.282278	-0.01	1.04

74321-12	0.282122	0.000126	0.819083	1.467980	0.000460	0.000808	0.000032	0.023830	0.000638	1109.8	40.34	0.282105	0.81	8.82
74321-13	0.282478	0.000057	0.883443	1.467301	0.000494	0.000895	0.000021	0.038151	0.001143	590.5	18.54	0.282468	1.94	3.97
74321-14	0.281998	0.000023	0.898163	1.467358	0.000186	0.000157	0.000007	0.005598	0.000147	524.6	16.22	0.281996	-16.23	1.64
74321-15	0.281533	0.000042	0.858402	1.466784	0.000888	0.001203	0.000016	0.045554	0.000598	1942.6	49.3	0.281488	-2.03	2.97
74321-16	0.282723	0.000028	0.858402	1.467537	0.000224	0.000797	0.000078	0.026518	0.001449	240.7	7.64	0.282719	3.01	1.96
74321-22	0.282842	0.000040	0.899465	1.467313	0.000301	0.001659	0.000049	0.062085	0.001857	274	8.94	0.282833	7.79	2.80
74321-23	0.281673	0.000040	0.829207	1.467182	0.000522	0.000985	0.000057	0.028946	0.001540	193.7	6.52	0.281669	-35.18	2.78
74321-25	0.282835	0.000022	0.915714	1.467274	0.000129	0.001176	0.000049	0.041245	0.002102	269.3	10.4	0.282829	7.54	1.52
74321-28	0.282274	0.000210	0.935404	1.468666	0.000733	0.003511	0.000266	0.118159	0.001657	288.3	12.94	0.282255	-12.34	14.68
74321-30	0.282333	0.000013	0.915092	1.467311	0.000186	0.000034	0.000002	0.001531	0.000071	553.3	23.82	0.282333	-3.66	0.94
74321-31	0.281818	0.000030	0.900889	1.467309	0.000186	0.000909	0.000027	0.032389	0.000279	1535.1	107.88	0.281791	-0.64	2.07
74321-32	0.281384	0.000018	0.905135	1.467290	0.000148	0.000799	0.000050	0.031294	0.002435	1862.5	63.16	0.281356	-8.58	1.27
74321-33	0.282421	0.000023	0.902604	1.467347	0.000170	0.000816	0.000045	0.032000	0.000930	480	21.66	0.282413	-2.46	1.64
74321-35	0.281934	0.000082	0.857529	1.467438	0.000544	0.001108	0.000026	0.029399	0.000539	1158.7	43.58	0.281909	-5.02	5.73
74321-38	0.282051	0.000015	0.899988	1.467278	0.000210	0.000094	0.000001	0.004329	0.000044	544.7	27.74	0.282050	-13.88	1.08
74321-39	0.280680	0.000089	0.942283	1.468607	0.000782	0.000668	0.000032	0.021008	0.001112	2976.1	138.34	0.280642	-8.03	6.23
74321-40	0.282055	0.000013	0.906179	1.467232	0.000199	0.000102	0.000001	0.004509	0.000029	509.9	30.3	0.282054	-14.53	0.93
74321-42	0.282778	0.000060	0.871961	1.467467	0.000457	0.000952	0.000047	0.029291	0.000689	923	46.72	0.282762	19.86	4.22
74321-44	0.282245	0.000032	0.874293	1.467284	0.000278	0.000917	0.000028	0.032002	0.001576	270.4	33.16	0.282241	-13.25	2.24

SUPPLEMENTARY TABLE 6: HF DATA COLLECTED FOR GNARLYKNOTS-1A, SAMPLE 74322

Sample Number	$^{176}\text{Hf}/^{177}\text{Hf}$	$2\sigma$	Hf fract	$^{178}\text{Hf}/^{177}\text{Hf}$	$2\sigma$	$^{176}\text{Lu}/^{177}\text{Hf}$	$2\sigma$	$^{176}\text{Yb}/^{177}\text{Hf}$	$2\sigma$	U/Pb Age (Ma)	$2\sigma$ Error	Hfi	$\epsilon\text{Hf}$	$2\sigma$ Error
74322-01	0.282332	0.000036	0.896914	1.467341	0.000247	0.001876	0.000114	0.070944	0.002138	1018	27.12	0.282296	5.51	2.50
74322-02	0.281351	0.000021	0.922065	1.467360	0.000168	0.000569	0.000010	0.021371	0.000432	493.5	14.42	0.281346	-39.94	1.46
74322-03	0.282113	0.000022	0.898463	1.467290	0.000227	0.000596	0.000005	0.021940	0.000168	1084.9	32.44	0.282101	0.10	1.55
74322-06	0.282095	0.000020	0.898803	1.467312	0.000200	0.000755	0.000007	0.028180	0.000410	1152.9	36.32	0.282079	0.86	1.37
74322-13	0.282973	0.000024	0.897319	1.467288	0.000213	0.000814	0.000030	0.026707	0.001324	131.3	4.64	0.282971	9.48	1.68
74322-16	0.282966	0.000019	0.895150	1.467240	0.000144	0.000496	0.000008	0.018127	0.000396	97.5	6.44	0.282965	8.54	1.31
74322-18	0.282417	0.000015	0.877702	1.467237	0.000257	0.000052	0.000001	0.002429	0.000056	591.5	18.06	0.282416	0.13	1.03
74322-20	0.281932	0.000016	0.887610	1.467289	0.000153	0.000793	0.000029	0.029069	0.001357	1565.1	42.5	0.281908	4.20	1.13

74322-21	0.283008	0.000018	0.862600	1.467247	0.000172	0.001010	0.000016	0.033485	0.000195	160.5	6.4	0.283005	11.33	1.24
74322-26	0.283016	0.000019	0.912286	1.467293	0.000180	0.000290	0.000013	0.008897	0.000363	100.8	8.28	0.283015	10.38	1.30
74322-27	0.282298	0.000019	0.913777	1.467358	0.000150	0.000885	0.000026	0.033197	0.000890	469.3	16.56	0.282291	-7.04	1.36
74322-29	0.282418	0.000014	0.913889	1.467274	0.000146	0.000052	0.000003	0.002172	0.000093	540.5	16.64	0.282417	-0.97	0.95
74322-31	0.282038	0.000028	0.902806	1.467349	0.000230	0.000614	0.000020	0.021820	0.001109	1134.3	36.62	0.282025	-1.49	1.99
74322-32	0.282096	0.000018	0.904417	1.467242	0.000159	0.001006	0.000044	0.037132	0.001386	1133	32.08	0.282075	0.26	1.24
74322-40	0.281603	0.000033	0.866871	1.467429	0.000338	0.000709	0.000004	0.030707	0.000956	1647.5	48.86	0.281581	-5.53	2.28
74322-42	0.282384	0.000037	0.825370	1.467421	0.000211	0.001446	0.000113	0.045311	0.002578	954.8	26.78	0.282358	6.27	2.57
74322-45	0.282685	0.000018	0.886207	1.467217	0.000192	0.000688	0.000042	0.024691	0.001232	320.8	11.36	0.282681	3.45	1.25
74322-50	0.283020	0.000019	0.899535	1.467255	0.000170	0.001008	0.000036	0.029498	0.000957	179.1	6.02	0.283016	12.16	1.36

SUPPLEMENTARY TABLE 7: HF DATA COLLECTED FOR GNARLYKNOTS-1A, SAMPLE 74323

Sample Number	176Hf/177Hf	2σ	Hf fract	178Hf/177Hf	2σ	176Lu/177Hf	2σ	176Yb/177Hf	2σ	U/Pb Age (Ma)	2σ Error	Hfi	εHf	2σ Error
74323-07	0.282430	0.000038	0.929782	1.467203	0.000144	0.000931	0.000032	0.034361	0.001148	1005.5	31.2	0.282413	9.34	2.65
74323-08	0.282871	0.000025	0.925638	1.467316	0.000155	0.001051	0.000016	0.040081	0.000256	100.2	6.2	0.282869	5.20	1.72
74323-09	0.281754	0.000017	0.922809	1.467248	0.000149	0.000128	0.000000	0.005280	0.000036	566.1	18.9	0.281753	-23.92	1.20
74323-10	0.281769	0.000015	0.929398	1.467267	0.000155	0.000120	0.000000	0.004897	0.000038	571.4	18.0	0.281768	-23.26	1.07
74323-11	0.282886	0.000019	0.922150	1.467221	0.000147	0.000551	0.000015	0.019603	0.000723	225.2	10.1	0.282883	8.48	1.31
74323-12	0.282302	0.000022	0.925129	1.467257	0.000186	0.000973	0.000025	0.036387	0.001186	984.7	27.2	0.282284	4.31	1.52
74323-13	0.282175	0.000017	0.931566	1.467304	0.000194	0.000236	0.000004	0.009878	0.000244	557.8	25.4	0.282173	-9.24	1.19
74323-14	0.282176	0.000017	0.939542	1.467312	0.000212	0.000254	0.000002	0.010690	0.000047	571.4	23.3	0.282173	-8.91	1.22
74323-15	0.282386	0.000017	0.930070	1.467247	0.000212	0.000438	0.000003	0.016815	0.000098	178.9	16.6	0.282385	-10.19	1.21
74323-19	0.282274	0.000020	0.940520	1.467239	0.000158	0.001135	0.000059	0.043380	0.002120	741.9	21.8	0.282258	-2.09	1.39
74323-20	0.282292	0.000019	0.954907	1.467240	0.000172	0.000746	0.000005	0.028806	0.000274	732.7	21.8	0.282282	-1.46	1.36
74323-22	0.282396	0.000018	0.939874	1.467284	0.000174	0.000492	0.000006	0.020412	0.000216	597.4	16.1	0.282390	-0.66	1.29
74323-30	0.282988	0.000040	0.932629	1.467142	0.000138	0.003087	0.000025	0.106831	0.001648	96.4	2.9	0.282983	9.13	2.81
74323-31	0.282957	0.000036	0.941798	1.467167	0.000173	0.001627	0.000012	0.056666	0.000235	95.1	4.6	0.282954	8.08	2.50
74323-40	0.281941	0.000018	0.931887	1.467213	0.000117	0.000512	0.000006	0.019464	0.000362	561.0	28.5	0.281935	-17.57	1.27
74323-41	0.282125	0.000015	0.928601	1.467231	0.000159	0.000130	0.000003	0.005634	0.000113	528.7	26.2	0.282124	-11.62	1.02
74323-63	0.282410	0.000019	0.909117	1.467247	0.000147	0.000721	0.000001	0.029415	0.000210	528.1	15.3	0.282402	-1.77	1.36

74323-64	0.282328	0.000012	0.908228	1.467201	0.000163	0.000051	0.000000	0.002545	0.000042	591.1	16.9	0.282327	-3.02	0.87
----------	----------	----------	----------	----------	----------	----------	----------	----------	----------	-------	------	----------	-------	------

SUPPLEMENTARY TABLE 8: HF DATA COLLECTED FOR GNARLYKNOTS-1A, SAMPLE 74326

Sample Number	176Hf/177Hf	2 $\sigma$	Hf fract	178Hf/177Hf	2 $\sigma$	176Lu/177Hf	2 $\sigma$	176Yb/177Hf	2 $\sigma$	U/Pb Age (Ma)	2 $\sigma$ Error	Hfi	$\epsilon$ Hf	2 $\sigma$ Error
74326-01	0.282079	0.000014	1.135225	1.467291	0.000178	0.000134	0.000001	0.004333	0.000059	1261.2	38.16	0.282075	3.19	0.95
74326-02	0.280795	0.000017	1.117271	1.467394	0.000218	0.000853	0.000025	0.029819	0.000807	2684	70.72	0.280751	-10.99	1.19
74326-03	0.282994	0.000015	1.121588	1.467181	0.000123	0.000800	0.000025	0.026683	0.001176	148.2	11.34	0.282991	10.59	1.06
74326-04	0.280963	0.000022	1.112096	1.467331	0.000285	0.000522	0.000017	0.019172	0.001066	2703.6	83.8	0.280936	-3.97	1.53
74326-08	0.282811	0.000023	1.117669	1.467185	0.000309	0.000748	0.000030	0.028824	0.001342	288.7	11.5	0.282807	7.21	1.61
74326-12	0.282461	0.000013	1.135316	1.467195	0.000169	0.000409	0.000001	0.015919	0.000201	528	16.82	0.282457	0.18	0.88
74326-14	0.282335	0.000013	1.138561	1.467242	0.000139	0.000209	0.000046	0.007813	0.001663	510.3	15.12	0.282333	-4.63	0.88
74326-16	0.281885	0.000015	1.127952	1.467313	0.000136	0.000269	0.000002	0.009787	0.000134	1128.3	38.88	0.281879	-6.77	1.03
74326-19	0.282298	0.000018	1.140682	1.467313	0.000156	0.000443	0.000003	0.016411	0.000219	726.2	28.66	0.282292	-1.22	1.28
74326-22	0.281674	0.000017	1.126622	1.467226	0.000204	0.000251	0.000003	0.009512	0.000168	513.9	22.18	0.281671	-27.97	1.22
74326-24	0.282348	0.000030	1.101726	1.467323	0.000214	0.000439	0.000051	0.013927	0.001214	650.2	25.02	0.282342	-1.16	2.09
74326-25	0.282161	0.000018	1.133673	1.467242	0.000177	0.000444	0.000061	0.017471	0.002519	895	32.92	0.282153	-2.34	1.28
74326-26	0.282321	0.000011	1.134009	1.467223	0.000198	0.000046	0.000001	0.002167	0.000046	558.8	24.42	0.282320	-3.99	0.77
74326-31	0.283025	0.000020	1.141671	1.467299	0.000193	0.000816	0.000028	0.024894	0.001017	98	4.74	0.283023	10.60	1.41
74326-34	0.282423	0.000026	1.136478	1.467302	0.000150	0.001555	0.000018	0.059029	0.000489	358.5	12.78	0.282413	-5.20	1.81
74326-38	0.282476	0.000025	1.131562	1.467238	0.000177	0.001273	0.000020	0.045205	0.001224	302.6	11.34	0.282468	-4.48	1.73
74326-41	0.282795	0.000021	1.115211	1.467256	0.000137	0.000715	0.000022	0.023437	0.000936	241.5	8.36	0.282792	5.61	1.46
74326-42	0.282338	0.000011	1.145011	1.467246	0.000117	0.000027	0.000002	0.001200	0.000086	565.5	19.54	0.282338	-3.21	0.74
74326-43	0.282818	0.000084	1.046049	1.467243	0.000318	0.001694	0.000075	0.044654	0.001507	242.7	8.5	0.282811	6.30	5.87
74326-44	0.282378	0.000020	1.135928	1.467259	0.000153	0.000178	0.000010	0.007010	0.000497	651.1	24.48	0.282376	0.06	1.38
74326-45	0.282290	0.000018	1.126072	1.467368	0.000302	0.000030	0.000002	0.001408	0.000071	503.7	17.98	0.282290	-6.29	1.25
74326-46	0.282273	0.000022	1.121694	1.467257	0.000207	0.000822	0.000064	0.028373	0.001501	771.7	28.02	0.282261	-1.30	1.56
74326-50	0.282510	0.000019	1.116452	1.467315	0.000255	0.000379	0.000031	0.013613	0.001180	537.5	19.5	0.282506	2.12	1.33
74326-51	0.280724	0.000025	1.101397	1.467250	0.000279	0.000225	0.000008	0.007927	0.000188	2370.3	91.62	0.280714	-19.63	1.76
74326-53	0.281766	0.000014	1.127142	1.467277	0.000126	0.000416	0.000012	0.015929	0.000424	558.4	23.38	0.281762	-23.77	0.97
74326-55	0.282403	0.000014	1.129301	1.467280	0.000177	0.000110	0.000022	0.003775	0.000656	530.9	19.64	0.282402	-1.73	1.01

74326-57	0.282366	0.000032	1.069338	1.467203	0.000603	0.000047	0.000005	0.001754	0.000118	503.9	22.22	0.282366	-3.61	2.21
74326-60	0.282532	0.000025	1.108738	1.467244	0.000124	0.002011	0.000066	0.074911	0.001722	285.8	11.24	0.282521	-2.99	1.75
74326-61	0.281680	0.000055	1.045607	1.467322	0.000412	0.001303	0.000063	0.036228	0.001182	1649.4	52.18	0.281640	-3.39	3.85
74326-66	0.282212	0.000026	1.138020	1.467184	0.000208	0.000591	0.000067	0.024845	0.002965	685.4	19.8	0.282204	-5.27	1.80
74326-71	0.282741	0.000070	1.101544	1.467138	0.000319	0.001086	0.000034	0.038287	0.000083	242.8	10.66	0.282736	3.68	4.87
74326-72	0.282304	0.000032	1.076299	1.467359	0.000336	0.000433	0.000034	0.016254	0.001573	765.7	21.94	0.282298	-0.14	2.21
74326-77	0.281398	0.000052	1.071156	1.467291	0.000407	0.000948	0.000102	0.034428	0.002638	1856.7	50.22	0.281365	-8.39	3.67
74326-78	0.282434	0.000021	1.140219	1.467216	0.000130	0.001334	0.000026	0.050635	0.001282	244.1	12	0.282428	-7.22	1.48
74326-79	0.282261	0.000035	1.116642	1.467169	0.000431	0.000692	0.000020	0.030204	0.000442	803.9	24.9	0.282251	-0.94	2.43